

University of Pécs
Faculty of Sciences
Institute of Chemistry

B.Sc. thesis

**Redox, kinetic, and photochemical properties of 2,5-dihydroxy-1,4-
benzoquinone, and other model systems**



Supervisor: Dr. Ósz, Katalin
Associate Professor
Department of Physical Chemistry and
Materials Science

Author: Nazir, Muhammad Zahid
BSc Chemistry
Neptun code: VOBJDP

Pécs, 2022.

“Surely in the creation of the heavens and the earth, and in the alternation of night and day, there are signs for men of understanding.”

(Quran 3:190)

Table of contents

Title page	1
Motivation	2
Table of contents	3
Chapter 1. Introduction	5
1.1. Properties and derivatives of 1,4-benzoquinones	7
1.2. Photochemistry of 1,4-benzoquinones	9
1.3. Cyclic Voltammetry and electrochemistry of 1,4-benzoquinones	11
1.4. Redox Flow Battery	13
1.4.1. Iron-Copper Redox Flow Battery	13
1.4.2. Benzoquinone Organic Redox Flow Battery	14
1.5. Diode-Array Spectrophotometer as a Photoreactor	16
Chapter 2. Materials and methods	18
2.1. Materials used	18
2.2. Measurement methods used	19
2.2.1. Cyclic Voltammetry	19
2.2.2. UV-Vis Spectrophotometry	19
2.2.3. Chemical equilibriums drawn in MEDUSA	20
2.3. Processing of data	20
Chapter 3. Results and discussion	21
3.1. Investigation of redox properties of Iron-Copper redox couple	21
3.2. Investigation of photo-decomposition of 2,5-dihydroxy-1,4-benzoquinone	29
3.3. Investigation of redox properties of 2,5-dihydroxy-1,4-benzoquinone	31

Chapter 4. Summary	36
Acknowledgement	38
Reference list	39
List of abbreviations	43
Appendixes	44
Declaration of originality	46

Chapter 1. Introduction

This conscious universe in which we live has always been a subject matter of study due to the inquisitive nature of mankind. Its Creator has embodied His signs in it such a way that curious people throughout the history connected the dots and discovered physical phenomena of nature. One of them was an energy source for the welfare of mankind. The irresponsible human activities throughout history have spoiled the sacred environment and now we are about to run out of fossil fuels. In this postmodern era with increasing demands for energy sources, we are in dire need of renewable and environmentally friendly energy sources.

Among the renewable energy sources, we have hydroelectric, biomass, geothermal, solar, and wind energies. The principle of solar energy is the utilization of electromagnetic radiation coming from the Sun naturally by converting and storing this energy using solar cells, solar vacuum tubes, artificial photosynthesis, and other convenient methods and devices. Several chemical compounds have been investigated and developed throughout the development of solar cells and energy storing devices. Benzoquinone derivatives are some of those compounds. They have their application from biological to physical processes.

We know that solar cells convert sunlight into electric energy by the photovoltaic effect, which is a physical and chemical phenomenon. But storing this converted energy with high efficiency and achieving higher energy density and retaining this potential for longer period, are the real ongoing research problems in the development of energy storing devices.^{1,2} In recent years, there has been an increasing trend to develop so-called "Organic Flow Batteries" that involve quinones as dissolved charge carrier of the electrolyte. The energy generation is based on photocatalyzed quinone redox couple ions conversion. The suitability of quinones in these systems is because they are involved in reversible redox reactions, are soluble in water, and the physical and the chemical properties of their system can be altered easily by varying the substituents on these quinones. Quinones containing these organic flow rechargeable batteries take advantage of this

reversible redox reaction and thus are an excellent way of converting photo-energy into electric energy.

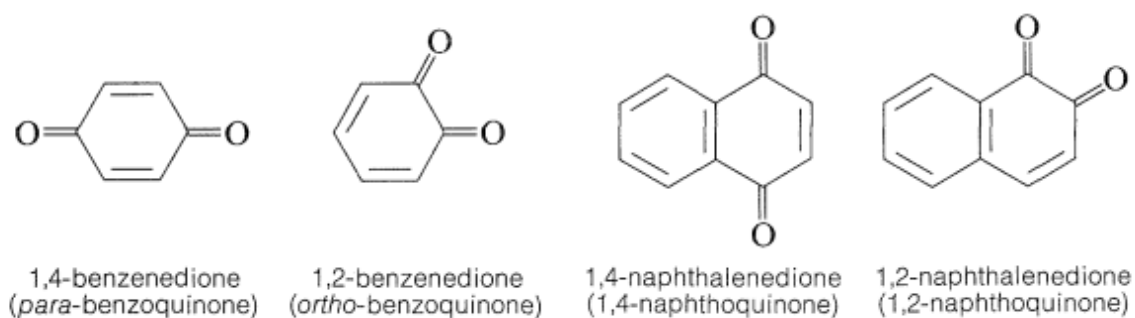
This thesis presents my research for my bachelor's thesis aiming at the possible utilization of solar energy by derivatives of photo-sensible 1,4-benzoquinone (BQ) molecule. The main purpose is to figure out whether the concerned substituted quinone is a right fit or not for the generation of photochemical energy that will ultimately be converted into electric energy. This can be achieved by investigation of photodissociation, kinetic and redox properties of these quinone derivatives.

It can be anticipated that by using appropriate quinone derivatives and right intensity of irradiation, we can increase the energy density, voltage and hence the efficiency of the cell. For my thesis, I have investigated hydroxy derivative of BQ which has not been investigated before for such specific redox, kinetic, and photochemical properties. This derivative is 2,5-dihydroxy-1,4-benzoquinone (BQ(OH)₂). Its photo-decomposed redox system was investigated by irradiating it with UV-Vis light on a diode-array spectrophotometer. The instrument photo-decomposed and measured the absorbance changes at the same time. Irradiations went hourly long so it makes it possible to derive some kinetic properties too. In parallel to spectrophotometric measurements to observe absorbance changes, cyclic voltammetry (CV) was done on each step of experiment to see any decomposition electro analytically. Both techniques helped to analyse reaction intermediates and final products of quinones photo-decomposition. The iron-copper redox couple was also investigated using CV as a comparison redox model for photo-decomposed BQ redox system. From the previously published research results we can anticipate that the possibility of using BQs, as redox charge carrier and in other various applications, is influenced by several properties of the given derivative. The properties derived already also encourage us to measure and systematize information about quinones containing as many different substituents as possible to find the optimal derivative.

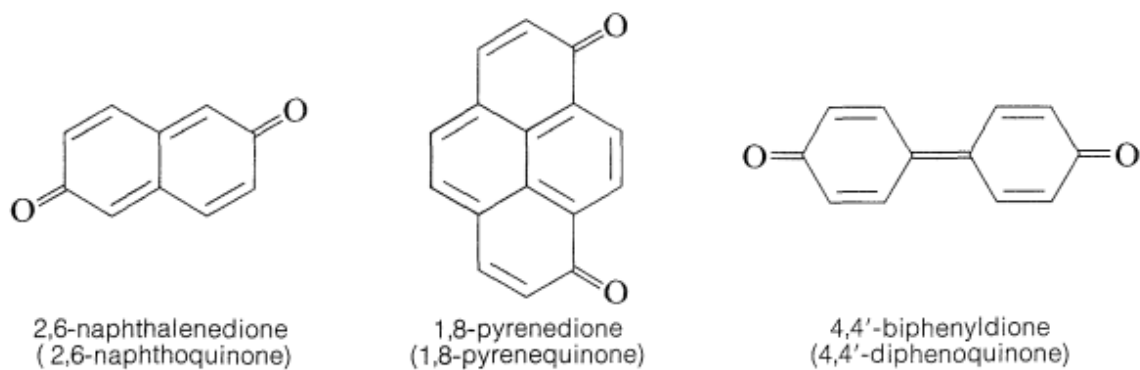
1.1. Properties and derivatives of 1,4-benzoquinones

Quinones are organic compounds which are usually derived from aromatic compounds by doing necessary rearrangements in their structures to get fully conjugated cyclic diones. They themselves are not aromatic compounds but conjugated cyclic diketones. The substituted benzoquinone family compounds are primarily based on 1,4-benzoquinone (BQ) which is oxidized derivative of 1,4-hydroquinone (H₂Q). They can also be obtained from other aromatic compounds e.g., from phenol by hydroxylation followed by oxidation. Natural occurrences of BQs are plants, lichens, fungi, and bacteria. From biological point of view, many BQ derivatives play important functions in biological systems like oxidative phosphorylation and photosynthetic electron transport chain.^{3,4}

A variety of quinone-like compounds have been known, the most common of them are in **Scheme 1**. Ortho-benzoquinones are difficult to prepare and are more reactive than para-benzoquinones. Among BQs, m-benzoquinone does not exist because its structure would be nonplanar, highly strained, and unstable, although some of its derivatives are known. In some quinones, arrangement of quinone ring extends over more than one ring called polycyclic quinones (**Scheme 2**).



Scheme 1: Most common benzoquinones.

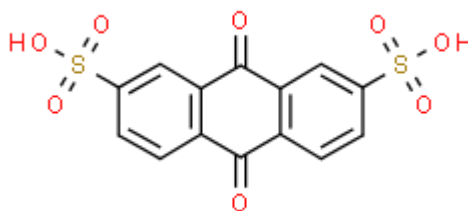


Scheme 2: Polycyclic quinones with two or more rings.

BQs have multifunctional properties of behaving in chemical environment like a ketone by forming oximes, an oxidant by forming dihydroxy derivatives, and an alkene by undergoing addition reactions.⁵ Strongly oxidizing agents among BQs include chloranil and 2,3-dichloro-5,6-dicyano-1,4-benzoquinone, also known as DDQ which is used for dehydrogenation of steroid ketones, alcohols, and phenols.

2,5-Dihydroxy-1,4-benzoquinone $BQ(OH)_2$, is one of the seven hydroxy derivatives of BQ. It is yellow orange solid having planer geometry and shows ferroelectric properties.⁶ It shows weak acid properties in solutions and its anions (e.g., $C_6H_2O_4^{2-}$ $pK_{a2} = 4.87$) can form variety of metal complexes by functioning as a binucleating ligand.⁷ It is the compound of investigation for this thesis regarding its photochemistry and redox properties. It is a compound of interest for scientists developing solar cells and charge carriers for flow batteries.

Some of the BQ derivatives have importance for their application as a charge carrier in metal-free redox flow batteries (RFB) such as 9,10-anthraquinone-2,7-disulfonic acid (AQDS) whose precursor can be found naturally in rhubarb, a spring vegetable.⁸ An AQDS aqueous RFB with inexpensive glassy carbon electrodes can yields a peak power density exceeding 0.6 W cm^{-2} at 1.3 A cm^{-2} with $> 99\%$ storage capacity retention per cycle which is very competitive in comparison to lithium ion batteries.⁸ These organic anthraquinone species can be synthesized from inexpensive chemicals easily and they are also free from metal toxicity.



Scheme 3: 9,10-anthraquinone-2,7-disulfonic acid (AQDS), a flow battery charge carrier.

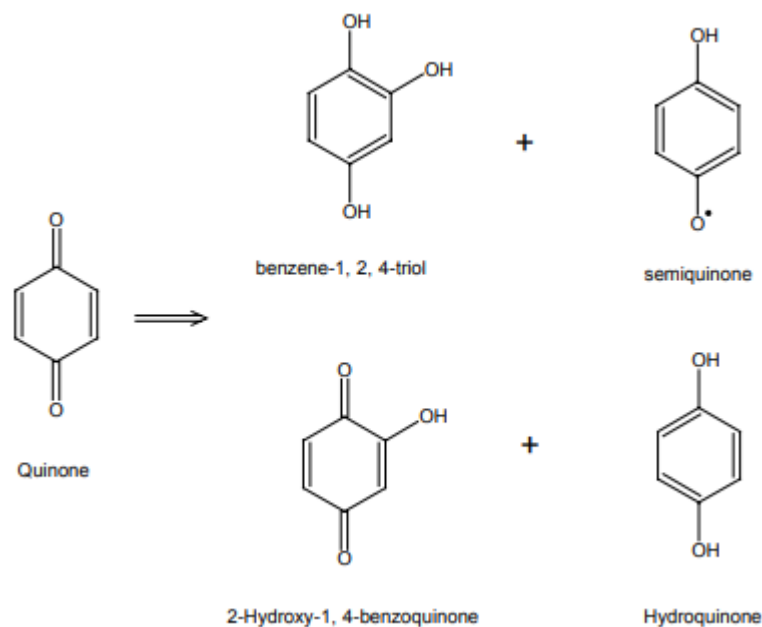
1.2. Photochemistry of 1,4-benzoquinones

Quinones are sensitive to light and their photo-decomposition takes place easily upon illumination. They are found widely both in biological and environmental systems as chromophores. Possible occurrences of quinone in environment which involve photo-degradation are lignin or microbial organic matter.

BQs and their derivatives contain conjugated pi-bond system such as C = C and C = O bonds. These bonds are responsible for σ , π and n type molecular transitions in these molecules. Upon illumination, these molecular orbitals go to excited states and electron transitions take place according to the incident wavelength. In the vacuum UV range (100-200 nm) $\sigma \rightarrow \pi^*$, in the UV range (200-400 nm) $\pi \rightarrow \pi^*$, and in the visible light range (400-800 nm), the $n \rightarrow \pi^*$ transitions are typical transitions for quinones. In the UV spectra, the aqueous solutions of BQs corresponds to three absorption bands $\pi \rightarrow \pi^*$, $\pi \rightarrow \pi^*$, and $n \rightarrow \pi^*$ transitions.⁹ The wavelengths of these transitions depend on the solvent and substitutions present on the BQ ring. After irradiation with UV, the ground state BQ molecules will be first excited to a singlet state and follow relaxation to the lowest excited singlet state. After this relaxation, it has been reported that most of BQs undergo rapid intersystem crossing to the excited triplet state. That is why due to their high intersystem crossing efficiency, it is accepted that BQ photochemistry originates from triplet state generally.¹⁰

The photolysis of BQ in the aqueous solution has already been identified long ago by chromatographic and spectrophotometric methods. From these studies, it

was discovered that the photo-decomposed products of BQ after irradiating it with UV-Vis light includes: benzene-1,2,4-triol, semiquinone, hydroquinone, and hydroxylated quinone (**Scheme 4**).



Scheme 4: Benzoquinone photoproducts.

In theory, four distinct mechanisms have been proposed that can produce these same products. These mechanisms are named as: the OH mechanism, direct triplet mechanism, intermediate product conversion mechanism, and quinone-quinone or electron transfer (at high quinone concentrations) mechanism. The study of these mechanisms has shown that when the aqueous BQ is illuminated with UV light, hydroquinone can be isolated partially as main product of the photo-decomposition and partially via intermediate benzene-1,2,4-triol and 2-hydroxy-1,4-benzoquinone. These intermediates get further converted directly or indirectly into suitable products that can yield energy. Theoretically, the triplet quinones by having strong oxidizing power, are capable of removing two hydrogen atoms from water molecule, and thus converting quinone to hydroquinone by releasing oxygen.^{11,12}

Because the final products for all these four mechanisms are identical, so product analysis cannot be a determining step to differentiate these reaction mechanisms. One of possible way is to distinguish between these mechanisms is to

test for the presence of a reaction intermediates. For this research gap, I proposed to conduct CV measurements to figure out peak potentials of reaction intermediates and photo-decomposed products. For my research goals, the quinone/hydroquinone conversion by releasing oxygen is also a favourable reaction in terms of solar energy utilization.

1.3. Cyclic Voltammetry and electrochemistry of 1,4-benzoquinones

The main part of my thesis results comprises cyclic voltammetry (CV) measurements for different solutions of quinones, and Fe/Cu solutions. So, I will describe briefly its concepts and applications in relation to quinones. CV is a very important potentiodynamic electrochemical technique widely used for electroanalytical analysis and sometimes it is called as „electrochemical spectroscopy”.¹³ It is mostly used in analysing redox processes to determine the stability of reaction products, finding intermediates in redox reactions,¹⁴ electron transfer kinetics,¹⁵ the reversibility of a redox reaction,¹⁶ corrosion measurements, and reduction potential range of the ions present in electrolyte which can be used for qualitative purpose and characterization of new compounds.¹⁷

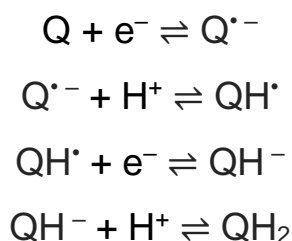
The experimental setup consists of a potentiostat, computer, and three electrode system (working, reference, and counter electrode). The working electrode's potential is ramped linearly versus time and driven between two limits (upper and lower limit) at a constant rate while the reference electrode remains at a constant potential. When the set limit is reached, the potential is reversed back at the same rate. The current is sampled at the end of each potential step. The upper and lower potential limits depend upon the choice of the solvent and the electrolyte. The current measured during the scan is plotted as a function of the potential of the working electrode to obtain the voltammogram.

The parameters that can influence voltammogram are scan rate, and applied potential range. Applied potential range also called as „potential window”, depends upon the analyte under study and decides the resolution of the scan while

the scan rate influences the redox activity at the working electrode (WE). Changing parameters like current threshold, concentration, and temperature also influence voltammogram indirectly. Altering these parameters will give us different set of data that can be used for analytical purposes for our analyte.

Oxidation occurs during the positive half of the scan, and an anodic current (i_{pa}) is measured. Similarly, reduction occurs during the negative half of the scan, and a cathodic current (i_{pc}) is measured. If the redox couple is reversible, the reduced analyte will begin to re-oxidize during the reverse scan, resulting in a reverse polarity current (anodic current). The more reversible the redox couple is, the more similar the oxidation peak will be in shape to the reduction peak. In this way, we can have information about redox potentials, reaction intermediates, and electrochemical kinetics for our analyte.

The electrochemistry of quinones has received a lot of attention due to their application for energy conversion and storage. One such example that I have mentioned previously is AQDS, a charge carrier for flow batteries (see **Scheme 3**). The reduction of BQ in aqueous solution has already been studied extensively by a lot of works and the mechanism of such reduction in aqueous solution can be summarized in **Scheme 5**.¹⁸ Reduction occurs via two successive one-electron transfers. In the first electron transfer, a single charge quinone radical-anion is formed which is further reduced and then second electron transfer happens which is followed by reduction to form hydroquinone finally.



Scheme 5: Mechanism for the reduction of benzoquinone in an aprotic solvent.

1.4. Redox Flow Battery

All over the world, the transition to renewable sources is flourishing at full pace and this makes stationary energy storage devices a pivotal to guaranteeing a reliable power source. Redox flow batteries (RFB) have become one of the priority topics of development by scientists and entrepreneurs in comparison to traditional lithium-ion batteries for storing solar and wind energy. This is because RFB are cost effective, environmentally friendly (free of toxic metal ions), durable, non-combustible, and can be used to store large amounts of energy over prolonged periods. Their response time is in the millisecond range, so they can be used in parallel circuits to manage energy quality and management efficiently and can even be incorporated into to electric grid.

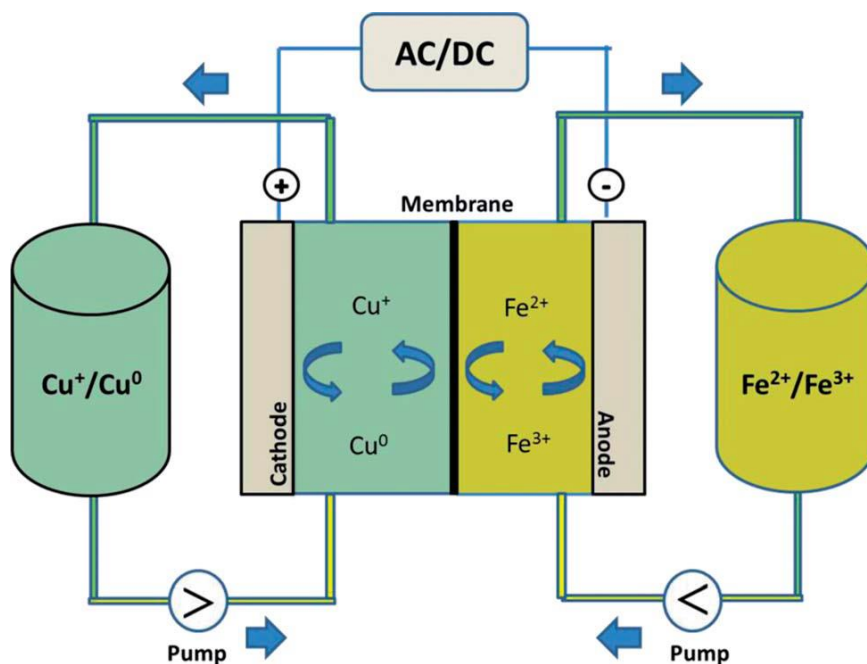
RFBs are electrochemical energy storage systems (rechargeable battery) which provides direct conversion between chemical and electrical energy. Chemical energy is driven by two chemical species dissolved in liquids as charge carrier that are pumped through the system on separate sides of a ion exchange membrane.

The concept RFB is almost half a century old but only the vanadium RFB invented by Skyllas-Kazacos et al. has been commercially available so far.¹⁹ From inorganic metal ions to organic quinones, a lot of RFBs with different charge carriers have already been developed. So, I have chosen to draw the critical review of iron-copper RFB and benzoquinone organic RFB in relation to my thesis. For their diversity of applications, acceptability by consumers for being cost effective, and environmental safety, we can anticipate their commercialization in near future at a large scale because more and more people are installing solar energy systems in houses.

1.4.1. Iron-Copper Redox Flow Battery

The first all-iron redox flow battery (Fe RFB) was invented by Hruska and Savinell in 1981.²⁰ It involved $\text{Fe}^{3+}/\text{Fe}^{2+}$ and Fe^{2+}/Fe redox couples in positive and negative electrolytes, respectively. Due to many limitations, it did not get succeeded to be

developed further. Recently, a new model has been developed that involve $\text{Fe}^{2+}/\text{Fe}^{3+}$ and Cu^+/Cu^0 as the positive and negative electrolytes, respectively (see **Scheme 6**). A standard cell voltage of 0.25 V was produced. During the charging cycle, Fe^{2+} are oxidized to Fe^{3+} in the positive half of cell, while Cu^+ are reduced to Cu^0 in the negative half of cell. When the battery is in the discharge cycle, reverse reactions happen.



Scheme 6: Illustration of a typical Fe/Cu RFB. ²¹

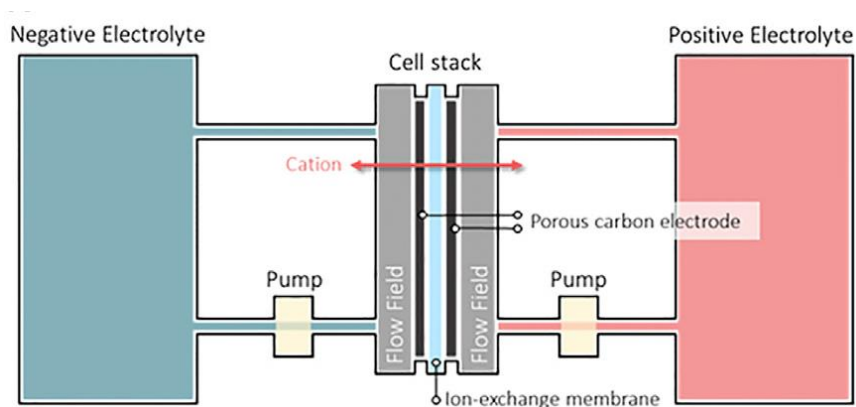
The main challenge in the development of the Fe/Cu RFB is its relatively low cell voltage and thus energy density. The cell voltage is significantly less than those of other RFB systems. However, by increasing the concentration of active charge carriers in the electrolyte, this issue can be resolved. The cost and abundance of both metals along with less toxicity than other metal RFBs (e.g., vanadium RFB) makes Fe/Cu RFB a topic of interest for further development.

1.4.2. Benzoquinone Organic Redox Flow Battery

The history of the development of quinone based flow batteries have gone through a lot of phases. Researchers have resolved a lot of challenges in their development not only about their design but also trying a lot of charge carriers and that is why

now we can see a list of BQ derivatives developed already for RFBs with varying characteristics. Some of RFBs are good for their output voltage and lag in energy density and response time while others have good energy density but not suitable due to low voltage. We must find middle ground in which we can have all optimal characteristics in a single model.

RFBs with quinones as redox active reactants, are potentially much less expensive than their vanadium RFBs counterpart. In addition, the chemical environment of these RFBs can be modified easily through selective functionalization. So, we can modify their aspects of performance such as voltage, energy conversion rate, and energy density according to the need.



Scheme 7: Schematic diagram of a typical Organic RFB. ²²

An organic-inorganic RFB based on 9,10-anthraquinone-2,7-disulfonic acid (AQDS) and HBr as electrolyte chemical species has already been developed. But the all-organic RFB gets preference over other types because it does not involve metals at all and its charge carriers are cheaper and easy to get from natural resources. One such example is all-organic AQDS-BQDS RFBs that involve quinone based redox couples at both electrodes.²³ The positive electrode in this RFB, is treated with 4,5-dihydroxybenzene-1,3-disulfonic acid (BQDS) and the negative electrode with anthraquinone-2,6-disulfonic acid (AQDS) separated by a proton permeable polymer membrane.

Some of the reported drawbacks of organic RFBs include a very complex system that makes it hard to maintain and low chemical stability because of the fact

that some organic molecules are prone to degradation reactions like nucleophilic substitution, and self-polymerization. These challenges can be resolved by deriving new properties, and investigating more and more substituents, and systematizing information about these quinones and their derivatives.

1.5. Diode-Array Spectrophotometer as a Photoreactor

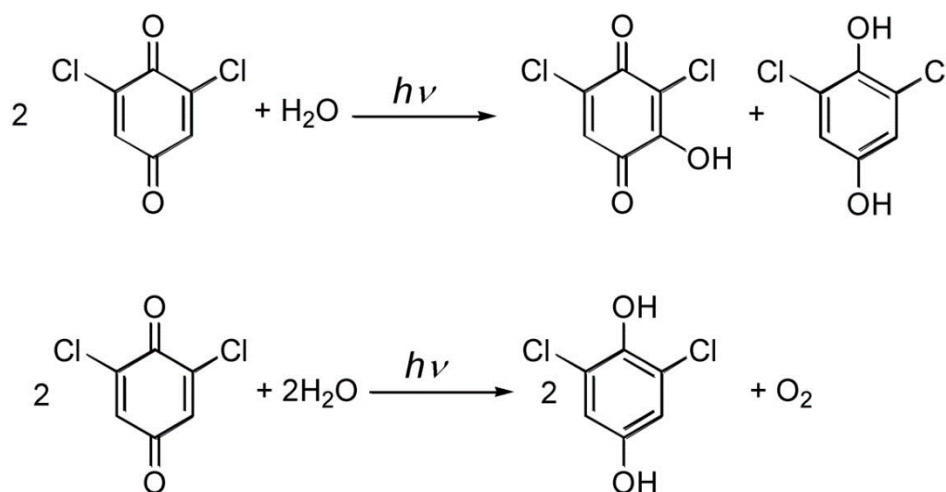
The use of modern spectrophotometers is a quality standard criterion in chemical trade and it stretch across various scientific fields from materials science, chemistry, and chemical engineering to biochemistry, and molecular biology. In the field of chemistry, spectrophotometers are mostly used for qualitative and quantitative determination, characterizing spectrum of compounds, and reaction kinetics etc.

However, some spectrophotometers can cause unexpected phenomena in solutions of photo-sensitive compounds as they can induce photochemical reactions due to absorption of light by the solution. These photo-induced processes must have to be taken into account otherwise we will get false observations for the analyte. It may sometimes lead to thermally induced reactions as well.²⁴ Alternatively, this property of spectrophotometers offers a number of new possibilities to study the kinetics of such photoreactions. For these measurements, a spectrophotometer acts as a photo-reactor and analysing unit at the same time. The basic concept of using these techniques works for both gas and liquid phases.²⁵ I have performed my photochemical experiments of BQ(OH)₂ in aqueous medium, so I found diode-array spectrophotometer as the right tool for testing my hypothesis in relation to quinones photo-decomposition and their kinetics.

Diode-array spectrophotometers are primarily based on the idea of a typical UV/Vis spectrophotometer but with the difference that diode-array spectrophotometers are optimized for rapid and simultaneous acquisition of a full band of UV/Vis spectrum.²⁶ This is achieved by designing the instrument in a way that polychromatic light is not dispersed until it passes the analyte, i.e., the monochromator is placed after the cell holder. In a diode-array spectrophotometer an intense polychromatic light passes through the analyte with enough energy for

inducing a photo-reaction. Commonly, in most of the instruments a deuterium and a halogen lamp are used and can cover 190-1100 nm of spectrum. After the precise experimental determination of the photon flux, the extent of the photoreaction can be quantified. But remember that there is no way in this experimental setup to monitor primary photo-reactions such as the formation of excited species, because the lifetime of such primary reactions are orders of magnitude shorter than the data acquisition rate of the spectrophotometer, but we can still excellently study the progress of photochemically induced reactions.

Lente et al. have already studied this phenomenon for 2,6-dichloro-1,4-benzoquinone (DCQ).^{25,27} In their experiments, they proved that diode-array spectrophotometer can be used as a photoreactor. The photo-induced chemical reactions in the aqueous solution of DCQ studied by Lente et al. are an excellent relevant example to my compound of study, BQ(OH)₂. For DCQ, photo-dissociation consists of the combination of two processes: the first is a water-assisted disproportionation of DCQ and second is the photo-reduction of DCQ by water.



Scheme 8: Photochemical splitting of DCQ on diode-array spectrophotometer. First is water assisted disproportionation reaction and second is photo-reduction of DCQ by water.

Chapter 2. Materials and methods

2.1. Materials used

A solution was prepared by dissolving 0.0845 g of solid $K_3[Fe(CN)_6]$, and 0.1056 g $K_4[Fe(CN)_6] \cdot 3H_2O$ in 50.0 cm³ of distilled H₂O in a volumetric flask. Each of solute in the solution has a molarity of 5.0 mM. The solute mixture solution was prepared on purpose to have a solution with oxidized and reduced species (Fe^{3+} , Fe^{2+}) at the same time so that it can serve as a redox system. Analytical grade 0.1 M $CuSO_4$ and 0.1 M $FeCl_3$ and their mixture solutions in different concentrations were prepared according to the need of each experiment. They were all obtained from *Sigma-Aldrich*. Doubly distilled water was used wherever dilution needed.

Solid 2,5-dihydroxy-1,4-benzoquinone ($C_6H_4O_4$) 98% (hereinafter as $BQ(OH)_2$) of analytical grade purity was used as a hydroxy derivative of 1,4-benzoquinone (BQ). It was purchased from *Alfa Aesar* company (Product: A11442). It was yellow orange in powdered state and when dissolved in water, it turned into a light red-orange solution. It was soluble in water but needed to be prepared on a magnetic stirrer because the solubility of BQ derivatives is affected by the type of substituents present on them. Those containing electron withdrawing groups takes longer to dissolve than those containing the electron donating group as their substituents.²⁸ $BQ(OH)_2$ contains electron withdrawing groups, so I accelerated the dissolution process using a magnetic stirrer. The concentration of stock solution of $BQ(OH)_2$ prepared was 1.0 mM. It was calculated from weight of $BQ(OH)_2$, and volume of the solution prepared. Due to photo-sensitive in nature, the stock solution was stored in a dark cabin to prevent any photoactivity.

H_2O_2 obtained from *Szkarabeusz Laboratóriumi, Vegyipari és Kereskedelmi Kft.* was used to oxidize the $BQ(OH)_2$ solution. Different concentrations like 3%, 10%, 20%, and 30% w/w were tried to figure out the right concentration of H_2O_2 for oxidation of $BQ(OH)_2$ solution. Due to degradability of H_2O_2 , new solution from stock bottle was used in each measurement.

2.2. Measurement methods used

2.2.1. Cyclic Voltammetry

For the cyclic voltametric (CV) measurements, 1.0 M NaCl was used as supporting electrolyte. The potentiostat *eDAQ ER466* used, was an integrated potentiostat with three electrode system to acquire electroanalytical data from our analytes. The 1.0 mm (OD 3 mm) glassy carbon disk electrode *eDAQ ET074* was used as working electrode (WE) and it was polished with alumina slurry before every measurement to get good peak results. Ag/AgCl electrode with 3.50 M KCl as electrode filling solution, was used as a reference electrode (RE). A third platinum wire electrode was used as counter electrode (CE). All these instruments for electroanalytical measurements were supplied by *eDAQ Pty. Ltd. Australia*. The parameters in each experiment are stated in the description of the given measurement results.

2.2.2. UV-Vis Spectrophotometry

Spectral changes were recorded for BQ(OH)₂ solutions before, during and after the reactions. The instrument used was double beam scanning UV-Vis spectrophotometer *A590* (S/N: UTC15J0010) supplied by *AOE Instruments Shanghai Co., Ltd.* The pathlength of the cuvette used was 1.00 cm and it was made up of quartz. The spectrums were recorded between 190-1000 nm wavelength.

Photochemical decomposition of BQ(OH)₂ into hydroxybenzoquinone and hydroquinone (hereinafter as BQ(OH) and H₂Q, respectively), was investigated by passing high intensity polychromatic UV-Vis light through the BQ(OH)₂ solution sample on a diode-array spectrophotometer acting as a photo-reactor and analysing unit at the same time. The instrument used was *Analytik Jena SPECORD S600* with two light sources, a deuterium lamp, and a halogen lamp operating in parallel. The host software controlling the instrument was *WinASPECT*. Kinetic and spectral measurements were performed at 24 ± 1 °C. The cuvette used in measurements was made up of quartz having a pathlength of 1.00 cm. It was placed in the cuvette holder with built-in magnetic stirrer to homogenize the solution. The spectrum was

recorded at 180-1100 nm, although it is sufficient to consider the spectrum range from 180-600 nm in the evaluation process because after 600 nm, there is almost zero absorbance. To pre-decompose the BQ(OH)₂ solution, a 6-watt *UVP UVGL-58 UV* lamp capable of emitting 254/365 nm wavelengths was used. The emitted photon flux of the lamp has a total photon energy of $\sum E = 2.98 \times 10^{-4}$ J/s and the total number of photons emitted were: $\sum N \text{ photon} = 7.72 \times 10^{14}$ photon/s.²⁹ BQ(OH)₂ solution was irradiated for 1 hour that gave the possibility to study the kinetics of the photo-decomposition.

2.2.3. Chemical equilibriums drawn in MEDUSA

It was necessary to interpret the equilibrium of iron-copper redox couple theoretically, especially in the presence of iron cyanide complexes, to see how the complexation situation changes between iron and copper when two solutions get mixed. Second, we mixed the solutions of iron and copper with Fe³⁺, Fe²⁺ and Cu²⁺ oxidation states in varying concentrations (1-10 and 10-1 V/V) in a series of measurements. So, in order to fully understand how cyanide ion will distribute itself among iron and copper during the redox process, we have simulated the equilibrium diagram of different possible soluble and insoluble chemical species formed in the solution using an algorithmic software called **MEDUSA** (making equilibrium diagrams using sophisticated algorithms) developed by *KTH Royal Institute of Technology, Stockholm, Sweden*.³⁰ I have made the equilibrium distribution diagram using this software which is based on literature data acquired through extensive experimentation.

2.3. Processing of data

The voltammograms of CV measurements were plotted in Microsoft Excel from the data files acquired from host controlling software application of the potentiostat. Similarly, spectrophotometric measurements graphs and comparative diagrams throughout this thesis were also made using Microsoft Excel.

Chapter 3. Results and discussion

3.1. Investigation of redox properties of Iron-Copper redox couple

For all cyclic voltammetry (CV) measurements, three electrode setup was used: 0.1 mm (OD 3 mm) glassy carbon disk working electrode (WE), platinum wire counter electrode (CE) and Ag/AgCl reference electrode (RE) having a standard reduction potential of 0.22 V vs SHE. Unbuffered 1.0 M NaCl solution was used as background electrolyte. The scan rates and potential ranges are given in caption of each voltammogram. The purpose of doing CV measurements for iron-copper redox couple was to study multicomponent redox system in comparison to redox system of benzoquinones.

From **Figure 1**, we can see the voltammogram of mixture solution of 5 mM $\text{K}_3[\text{Fe}(\text{CN})_6]$ and 5 mM $\text{K}_4[\text{Fe}(\text{CN})_6]$. The peak potentials do not change despite changing the scan rate. Only peak current values are increased with increase in scan rate. It is concluded that there is direct relationship between scan rate and peak current values (see **Figure 2**). It also implies that if the sample concentration is too low, then by increasing the scan rate, we can increase the intensities of peaks and it will make peaks more visible in CV. The voltammogram looks reversible, well measurable, and $\text{Fe}^{3+}/\text{Fe}^{2+}$ redox couple seems having one electron transition.

From **Figure 2**, we can infer an almost linear relationship between scan rates and peak current values. But, the plot starts a bit steeply and then saturates and becomes constant. It means that after a given scan rate, there is no point to increase it further because after a given value of scan rate, the intensity of the peak current will not increase anymore.

Figure 3 depicts the voltammogram for 0.1 M CuSO_4 . The cathodic and anodic peaks are very distant from each other. We can see here again the direct relationship between scan rates and peak current values. The voltammogram looks reversible, well measurable, and redox couple seems having two electron transition in a single jump. However, the slower scan rate is more accurate in comparison to higher scan rate because we can see peaks at very end of the potential window. In the case of higher scan rates, it becomes less precise.

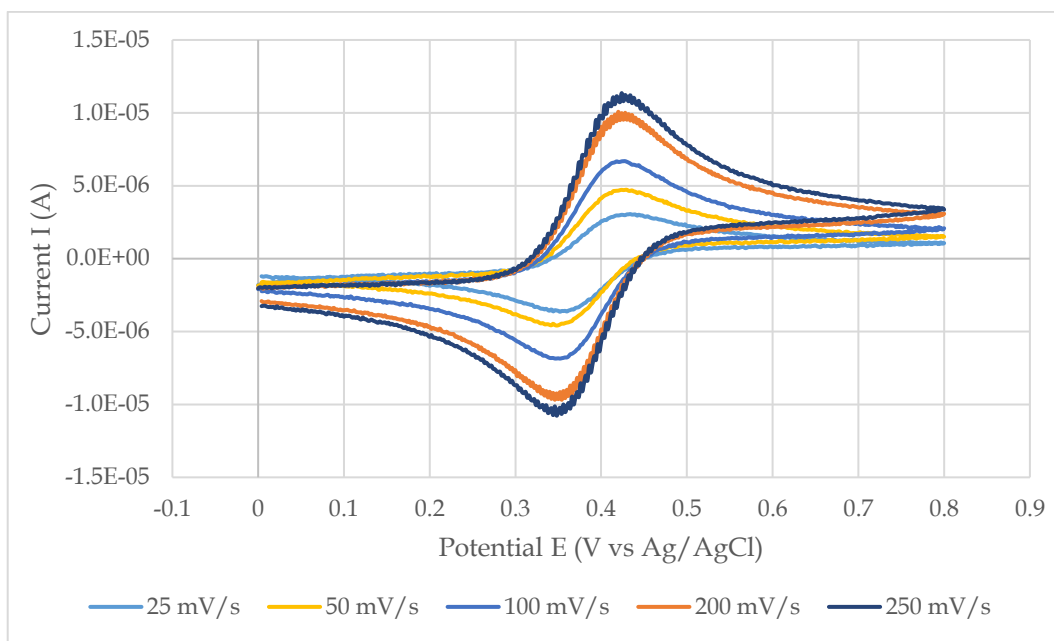


Figure 1: Cyclic voltammogram of solution containing 5 mM $K_3[Fe(CN)_6]$ and 5 mM $K_4[Fe(CN)_6]$. Scan is ramped from 0 to 0.8 V vs RE in positive direction. The Fe^{3+}/Fe^{2+} redox couple contains single electron transition. Scan rates (given in the figure legend) varied from 25 to 250 mV/s with $20\mu A$ current sensitivity range at 25 °C.

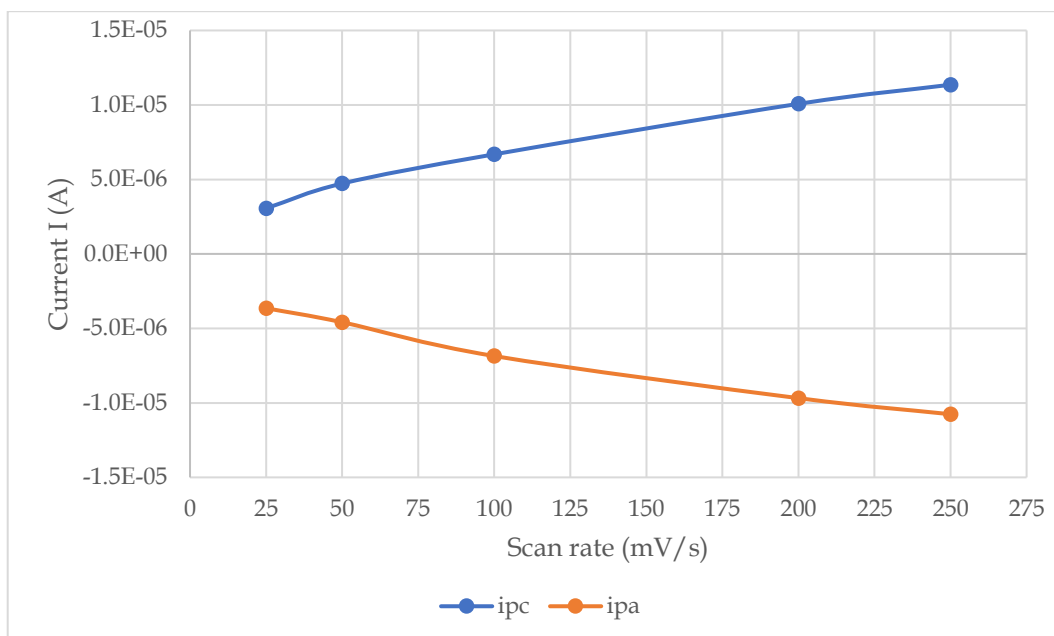


Figure 2: Peak potentials of Fe^{3+}/Fe^{2+} redox couple (from Figure 1) plotted versus scan rates.

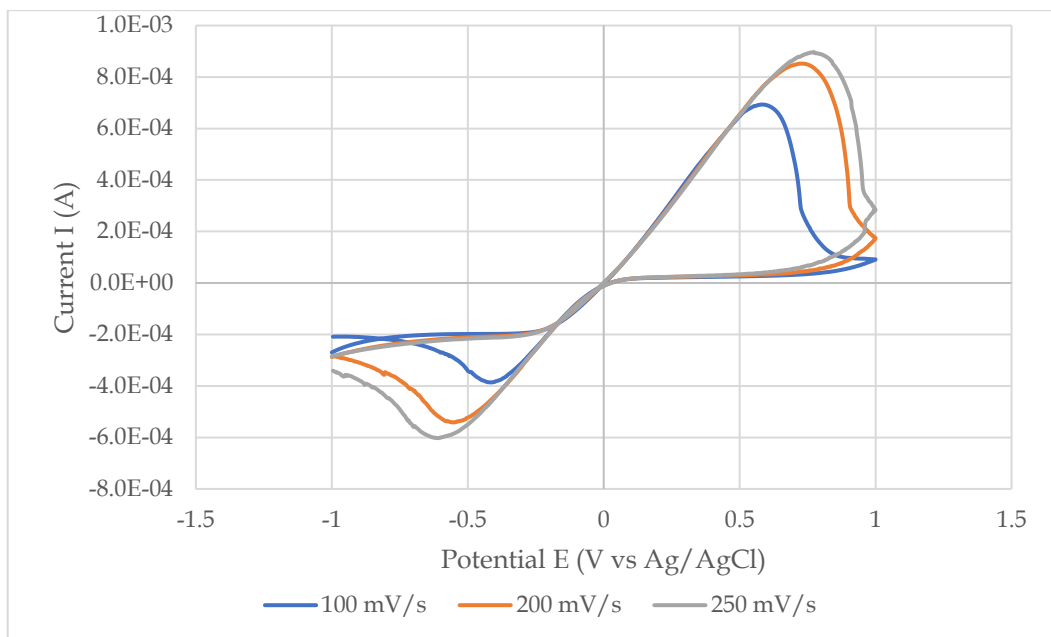


Figure 3: Cyclic voltammogram of 0.1 M CuSO₄. Scan is ramped from -1 V to +1 V vs RE in positive direction. Scan rates varied between 100 to 250 mV/s with 1 mA current sensitivity range at 25 °C.

The Cu²⁺/Cu_(s) redox couple seems having a two-electron transition in single jump as inferred from standard redox potentials calculated in Table 1.

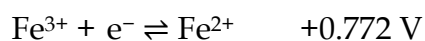


Table 1: Standard redox potentials calculated from peak potentials.

Scan (mV/s)	K ₃ [Fe(CN) ₆] + K ₄ [Fe(CN) ₆]		CuSO ₄	
	<i>E</i> _{pa} (V)	<i>E</i> _{pc} (V)	<i>E</i> _{pa} (V)	<i>E</i> _{pc} (V)
—				
25	0.352	0.434		
50	0.348	0.430		
100	0.352	0.428	-0.375	0.558
200	0.354	0.420	-0.542	0.692
250	0.348	0.424	-0.620	0.780
Average	0.351	0.427	-0.512	0.677
<i>E</i> _{1/2} (V)	0.389		0.082	
<i>E</i> ₀ (V)	0.609		0.302	
Literature value (V)	0.772		0.337	

We have used the peak potential values to calculate the half-potential and then the standard reduction potential for $\text{Fe}^{3+}/\text{Fe}^{2+}$ and $\text{Cu}^{2+}/\text{Cu}_{(s)}$ redox couples. (See **Table 1**). The experimental values are 0.609 V and 0.302 V in the case of $\text{Fe}^{3+}/\text{Fe}^{2+}$ and $\text{Cu}^{2+}/\text{Cu}_{(s)}$ redox couples, respectively. These small variations in redox potentials with respect to literature values may be caused by impurity in analyte or some instrumental or experimental error.

The voltammogram of mixture solution (1:1 v/v) of 0.1 M CuSO_4 with 0.5 mM $\text{K}_3[\text{Fe}(\text{CN})_6] + \text{K}_4[\text{Fe}(\text{CN})_6]$ solution (**Figure 4**) looks like the addition of previous two voltammograms (**Figure 1** and **Figure 3**). We can clearly see somewhat distorted $\text{Cu}^{2+}/\text{Cu}_{(s)}$ redox pair voltammogram in it. This distortion is caused by the presence of $\text{Fe}^{3+}/\text{Fe}^{2+}$ ions in the solution. But mainly the copper is dominant in the measured voltammogram.

Figure 5 summarizes all the three voltammograms of iron, copper, and mixture solution in a comparative way. It can be seen that the mixture solution voltammogram is more similar to copper than iron solution voltammogram. Peak intensities for the mixture solution are low and somewhat between the peaks of the others two voltammograms.

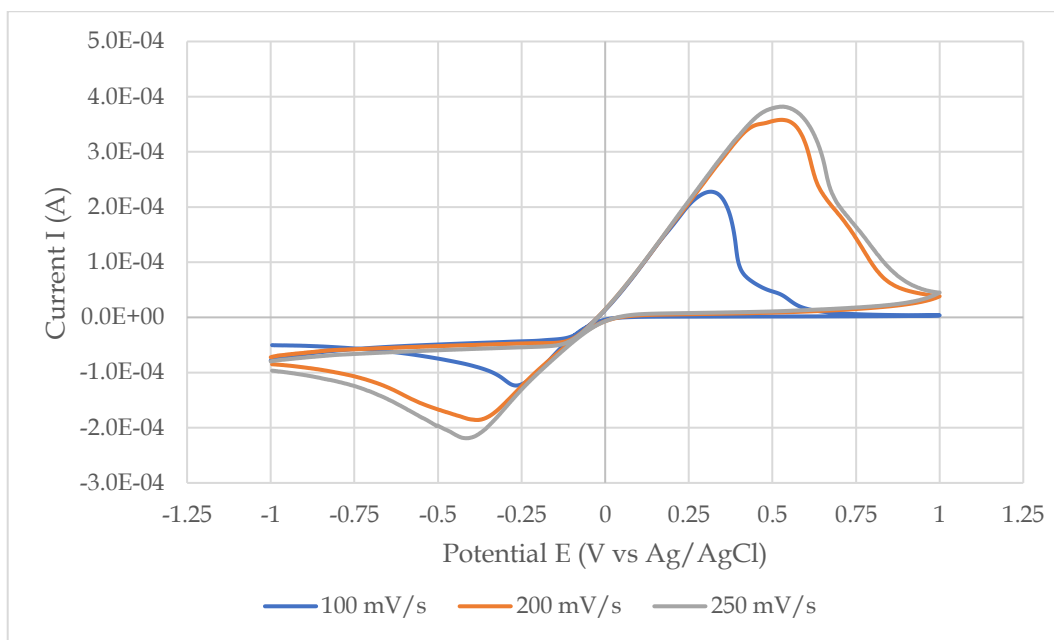


Figure 4: Cyclic voltammogram of mixture solution (1:1 v/v) of 0.1 M CuSO_4 and 0.5 mM $\text{K}_3[\text{Fe}(\text{CN})_6] + \text{K}_4[\text{Fe}(\text{CN})_6]$ solution. Scan is ramped from -1 V to +1 V vs RE in positive direction. Scan rates varied between 100 to 250 mV/s with 500 μA current sensitivity range at 25 $^\circ\text{C}$.

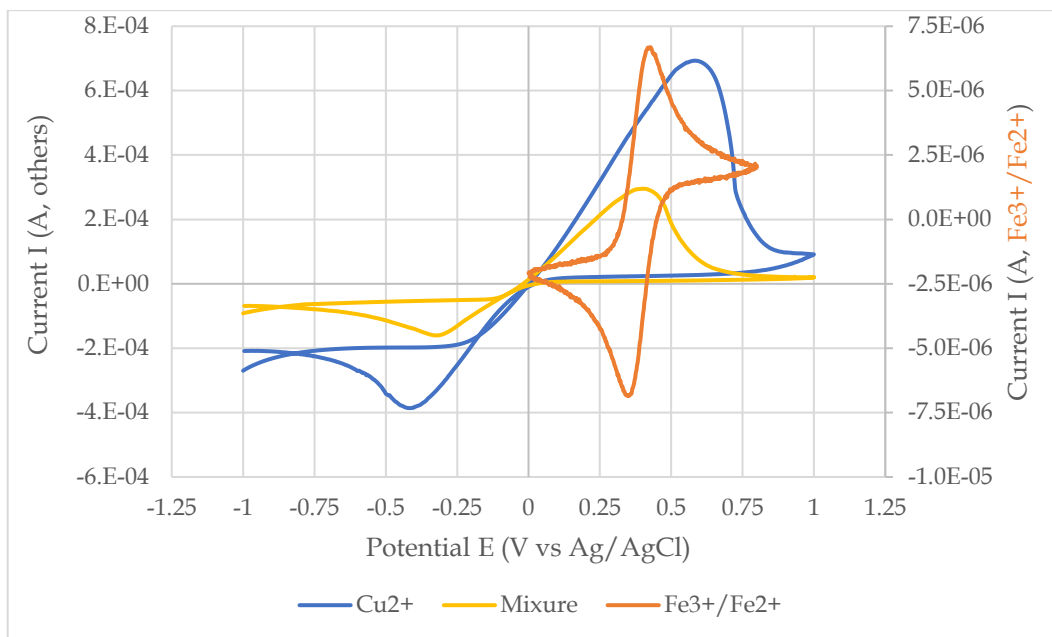


Figure 5: Comparison of voltammograms (Figures 1, 3, and 4) for 0.5 mM $K_3[Fe(CN)_6]$ + $K_4[Fe(CN)_6] \cdot 3H_2O$ solution with 0.1 M $CuSO_4$, and mixture solution (1:1 v/v).

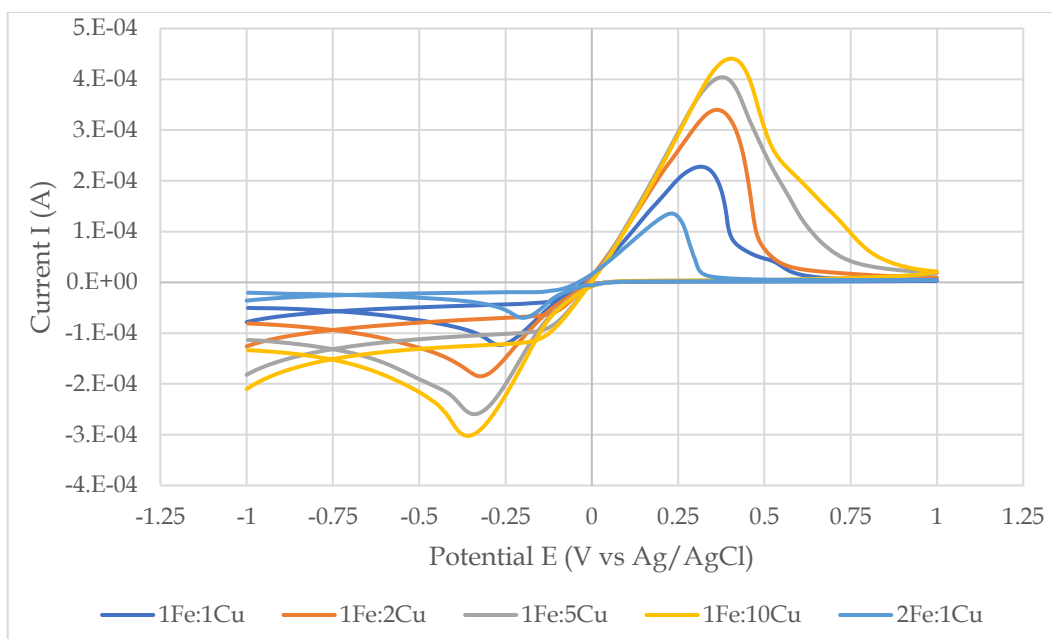


Figure 6: The effect on voltammogram by change in relative concentration of $CuSO_4$ and iron-cyanide complexes mixture solution.

From **Figure 6** we can infer that as we increase the concentration of the copper solution, the shape of CV becomes more and more similar to the pure copper solution and if we start increasing the iron concentration, then the CV of the mixture solution tends to look more like the iron one.

To understand more deeply the equilibrium processes in the mixture solution, a distribution diagram was calculated using literature stability constant and solubility constant data. The results are shown on **Figure 7**:

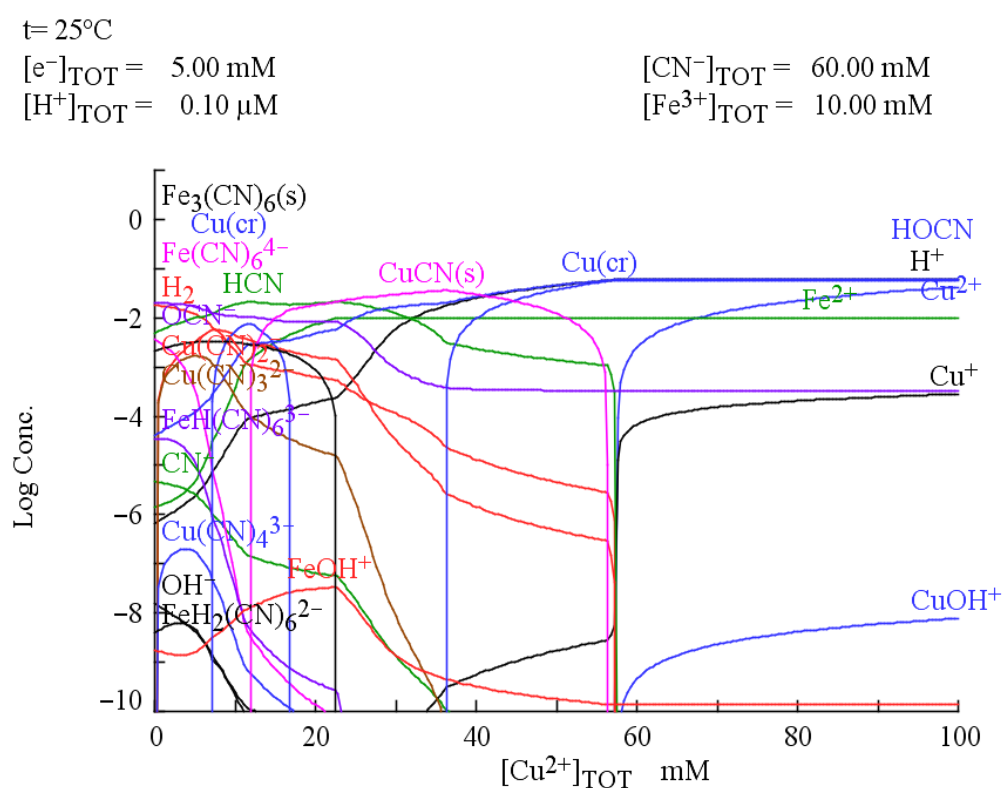


Figure 7: Equilibrium distribution diagram of CN⁻ ions in solution mixture of 0.1 M CuSO₄ and 5 mM K₃[Fe(CN)₆] + K₄[Fe(CN)₆].3H₂O solution. (Plotted with MEDUSA)

Here the concentration values for the different components were plotted on an algorithmic software (MEDUSA) to see the change in complexation situation of CN⁻ ions among different iron and copper ions as soon as we added CuSO₄ into the iron-complexes solution. The distribution of different soluble and insoluble species can be seen in the figure. In the beginning, CN⁻ is in high concentration with the

Fe²⁺ in form of [Fe(CN)₆]⁴⁻ and some other complexes. By increasing the Cu²⁺ concentration, CN⁻ gets replaced from Fe²⁺ and we have Cu(CN) copper(I) complex which is a solid but its concentration is low (not that Cu²⁺ is reduced by cyanide ions into the lower oxidation state of +1). It can cause precipitation if it appears in solution in high concentration. Then, Cu(CN)_(s) disappears and we can see crystalline Cu become the dominant component. Then, in the end we have all Cu²⁺ but we still have Cu⁺ in small amount. We can infer from it that when Cu²⁺ concentration is in excess, we usually have Cu²⁺/Cu⁺ redox system and some of the very little copper in CuOH⁺ form as hard as traceable.

From the point of voltammetry, we can conclude from this ions distribution that in case of Fe³⁺/Fe²⁺ redox system, the other ions present in the solution can substantially affect the redox potential and the shape of the voltammogram. Both the Fe³⁺ and Fe²⁺ ions like to be in a complexed form in the solution depending on which complexing agents are available. It is also a known fact that when we are measuring redox potentials, then only the free Fe³⁺ and Fe²⁺ ion concentrations are measured. Hence, redox potentials will be affected substantially by the ligands even if we keep the metal ions or metal ion pairs (two different oxidation states) the same.

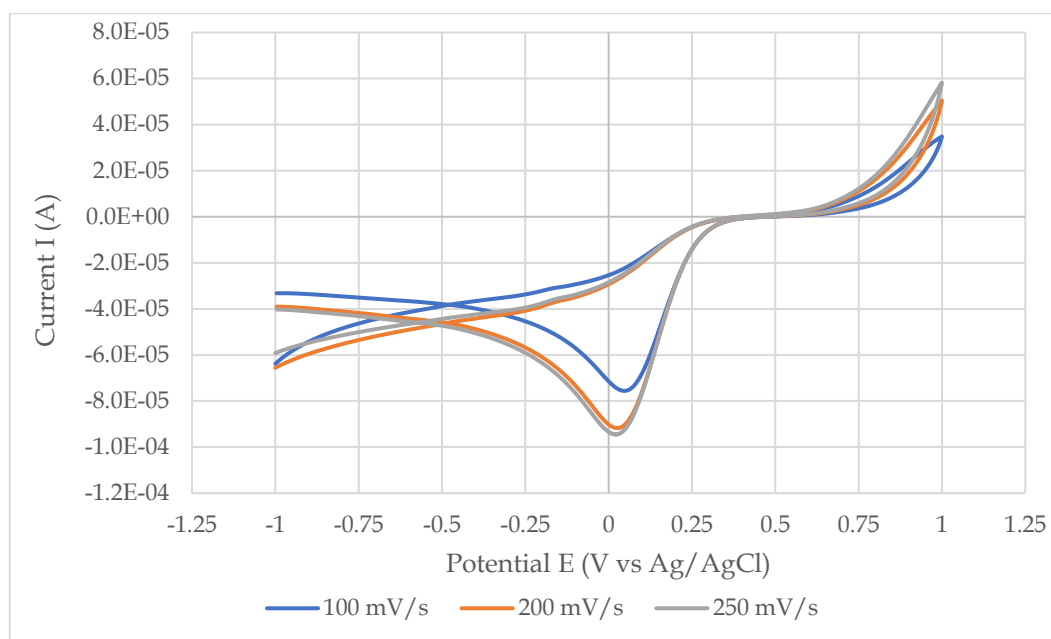


Figure 8: Cyclic voltammogram of 0.1 M FeCl₃. Scan is ramped from -1 V to +1 V vs RE in positive direction. Scan rates varied from 100 to 250 mV/s with 100 μ A current sensitivity range at 25 $^{\circ}$ C.

FeCl_3 with CuSO_4 was investigated as an alternative model to copper with iron-cyanide complexes model. **Figure 8** depicts the voltammogram of 0.1 M FeCl_3 . We can see an intense anodic peak at 0.05 V but the cathodic peak is blunt and not well visible. The voltammogram of CuSO_4 has already be described previously (see **Figure 3**).

From **Figures 9 and 10**, we can see the comparison of voltammograms of 0.1 M FeCl_3 , 0.1 M CuSO_4 and their mixture solution (1:1 v/v). We can see that there is an intense positive peak from copper at 0.6 V and an intense negative peak of iron at 0.06 V in very close positions. If we add these two peaks mathematically, then it will get double peak at 0.13 V and 0.4 V (mixture solution) somewhere in between the other two. If the concentration of the Fe would be increased, it will go towards Fe negative peak. And if the concentration of Cu is increased, then, towards the positive Cu peak.

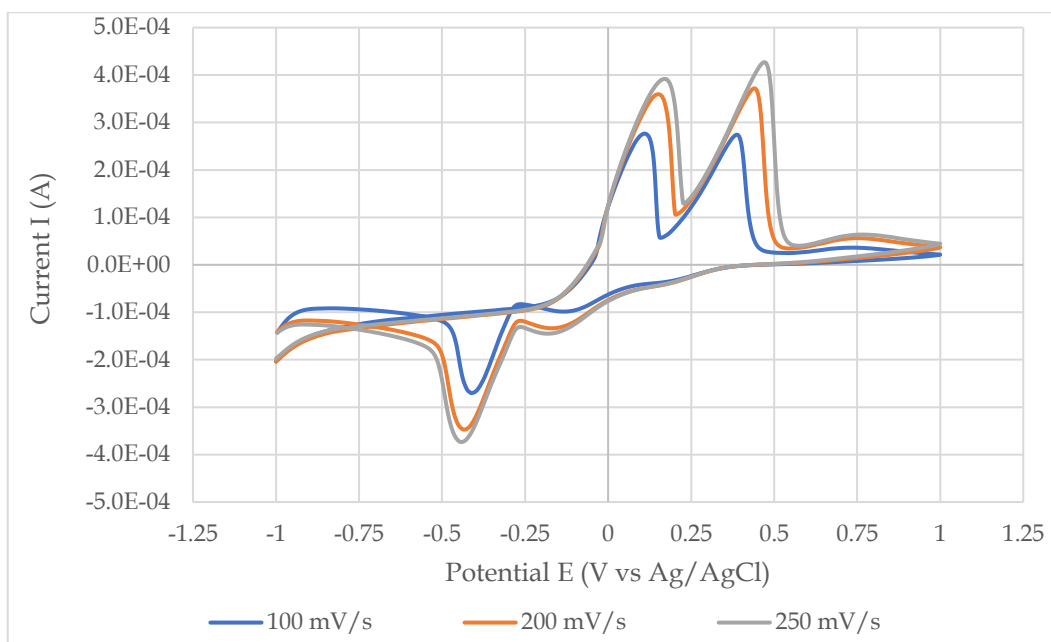


Figure 9: Cyclic voltammogram of mixture solution (1:1 v/v) of 0.1 M FeCl_3 and 0.1 M CuSO_4 . Scan is ramped from -1 V to +1 V vs RE in positive direction. Scan rates varied between 100 to 250 mV/s with 500 μA current sensitivity range at 25 °C.

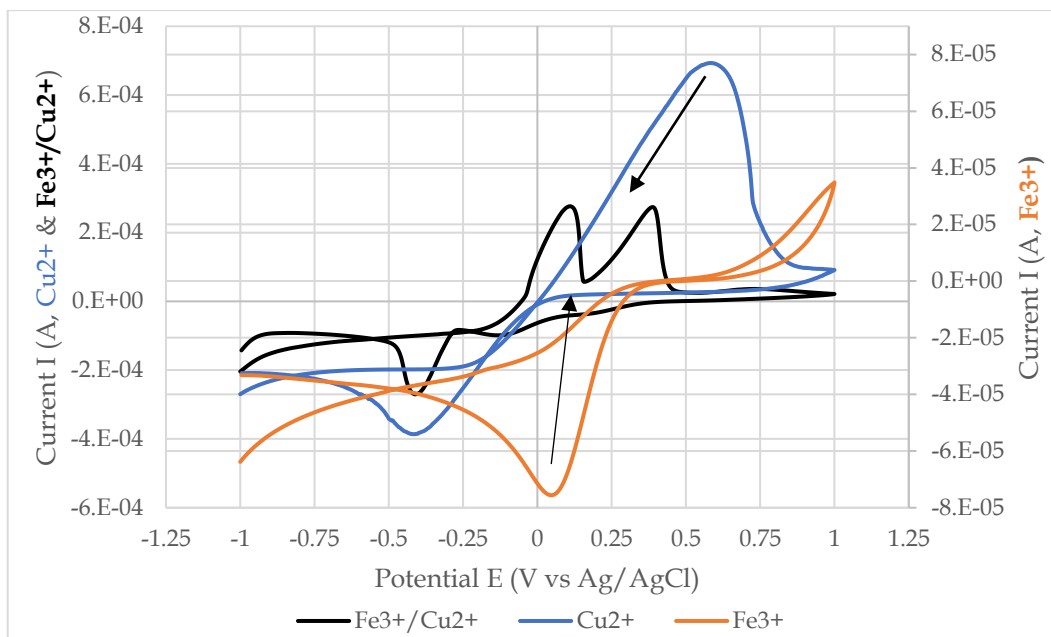


Figure 10: Comparison of voltammograms (Figures 3, 8, 9) for 0.1 M FeCl_3 , 0.1 M CuSO_4 , and their mixture solution (1:1 v/v).

3.2. Investigation of photo-decomposition of 2,5-dihydroxy-1,4-benzoquinone

The absorption spectrum of a freshly prepared 1.0 mM aqueous solution of BQ(OH)_2 was recorded by a scanning UV-Vis spectrophotometer before and immediately after irradiation for one hour on a diode-array UV-Vis spectrophotometer with the aperture shutter always open. A slight absorption band was observed at 477.5 nm. (see **Figure 11**) Based on the measured spectra, it can be stated that the diode-array spectrophotometer acted as photoreactor and photo-decomposed the BQ(OH)_2 sample. However, the conversion of the reaction is low even after an hour-long irradiation

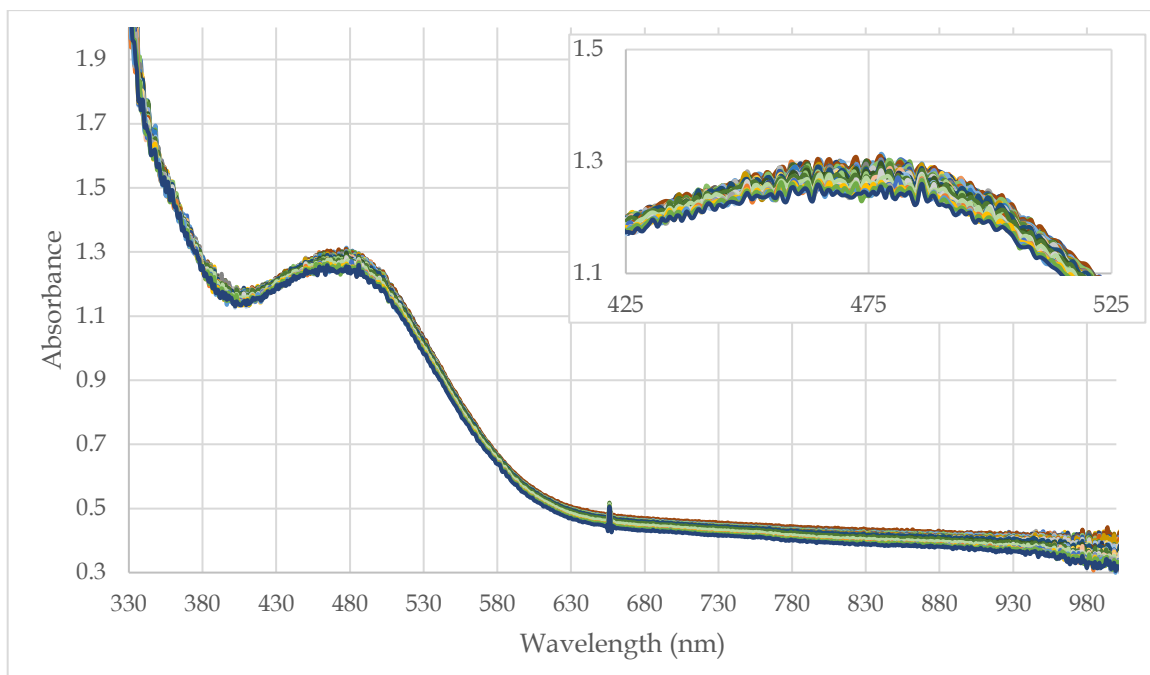


Figure 11: Irradiation spectrum of 1.0 mM BQ(OH)₂ solution illuminated for 1 hour using Analytik Jena SPECORD S600 diode-array spectrophotometer with 6-watt 365 nm UV lamp. Absorption band at 477.5 nm depicts slight photo-decomposition.

From the kinetic plot (**Figure 12**), i.e., the absorbances observed at 477.5 nm throughout one hour of illumination it can also be seen that the photo-decomposition reaction was quite slow. That means there is no substantial decomposition in BQ(OH)₂ solution under these conditions. Absorbance before irradiation was 1.31 and the final is 1.26 which means only 3.8% absorbance decrease after 1 hour of illumination which is not a big change.

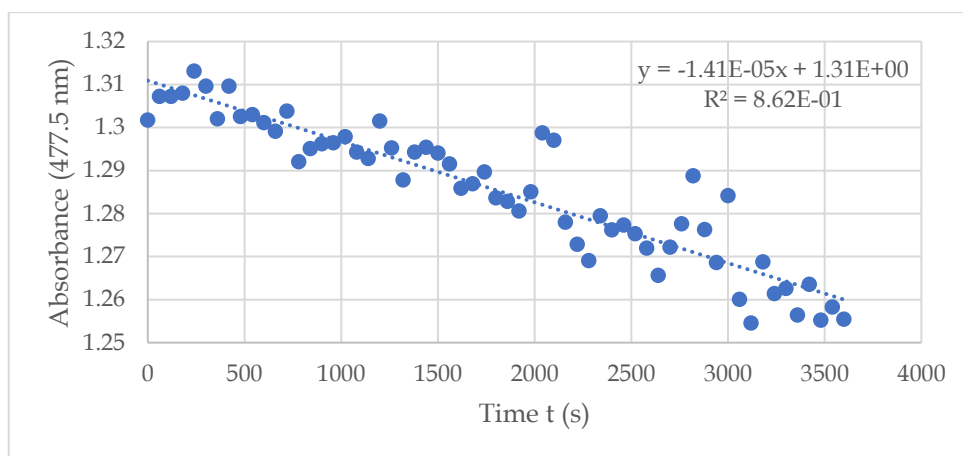


Figure 12: Kinetic plot of absorbance by BQ(OH)₂ at 477.5 nm

The absorbance decreases as well when the sample is illuminated by a 6-watt UVP UVGL-58 UV lamp. This lamp has a similar photon flux than the polychromatic light sources of the diode array spectrophotometer, however, the UV light of this lamp is more capable to drive the reaction because the absorption of the BQ(OH)₂ solution is much higher in the UV range than in the Vis.

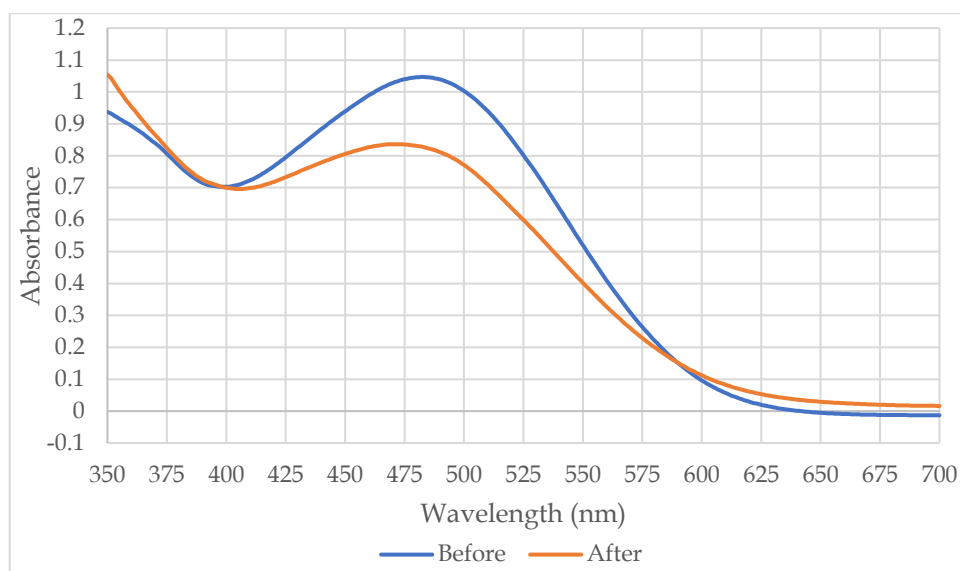


Figure 13: Absorption spectra of 1.0 mM BQ(OH)₂ solution before and after one hour of illumination by a 6-watt UVP UVGL-58 UV lamp.

For full decomposition, it will require much longer time for illumination, and an even more intense UV lamp. A higher value of absorbance means that the quinone will have higher chance for photochemical decomposition. Our idea is to charge the flow batteries from sunlight by capturing photons as much as possible. By combining the idea of quinones as photons capturers and charge carrier at the same time can increase the efficiency exponentially for RFB system. However, to use quinones for such purposes, not only the photochemical properties but also the redox properties of these solutions should be investigated.

3.3. Investigation of redox properties of 2,5-dihydroxy-1,4-benzoquinone

The cyclic voltammetry of BQ(OH)₂ was studied in its 0.1 mM aqueous solution. First, I performed CV measurement, then irradiated it on diode-array

spectrophotometer and finally conducted CV measurement again in order to derive some redox information due to photo-decomposition.

Figure 14 illustrates the voltammograms before and after irradiation. We can observe some concentration changes by comparing the two voltammograms. Concentration change means the amount of the original compound is decreased in the photoreaction. Before the illumination, we have a big peak at 0.2 V. After the illumination, the appearance of new peaks is observed at -0.18 V and 0.40 V in the forward scan. The forward peak at 0.40 V probably belongs to one of the products of the photo-decomposition reaction. The literature suggests this product should be hydroxyquinone and the -0.18 V peak belongs to quinone/hydroquinone. The quinone/hydroquinone are redox pair and just differs in some electrons. They can be interconverted by oxidation and reduction due to the presence of protons in the aqueous solution.

It would be a great idea to use oxidizing compound like H_2O_2 in right amount to produce hydroxyquinone with well visible peaks. Then, we can measure its pure CV voltammogram and say with certainty that the newly appeared peak belongs to hydroxyquinone. This could be a good step forward.

From **Figure 15**, we can infer that there is no effect of changing scan rate on the voltammogram of $\text{BQ}(\text{OH})_2$. Just the intensities of the peaks are increased that we have already observed in the case of iron-copper redox couple CV measurements (see **Figures 1-3**). Similarly, in the case of increasing current sensitivity range, we see no effect on CV measurement (**Figure 16**).

Figure 17 illustrates the effect of changing concentration by diluting the $\text{BQ}(\text{OH})_2$ solution. I started from 0.1 mM stock solution and measured its CV, then kept it diluting to decrease its concentrations and measuring CVs. After 0.09 mM concentration, the signal disappeared. It is because dilution reaches the micromolar range. The sensitivity of CV measurements is not so high for such low concentration ranges of quinone solutions. It becomes unreliable to measure CV. **Figures 19-21** in **Appendix A**, are the voltammograms for H_2O_2 . We have observed no change by changing the scan rate or current sensitivity range.

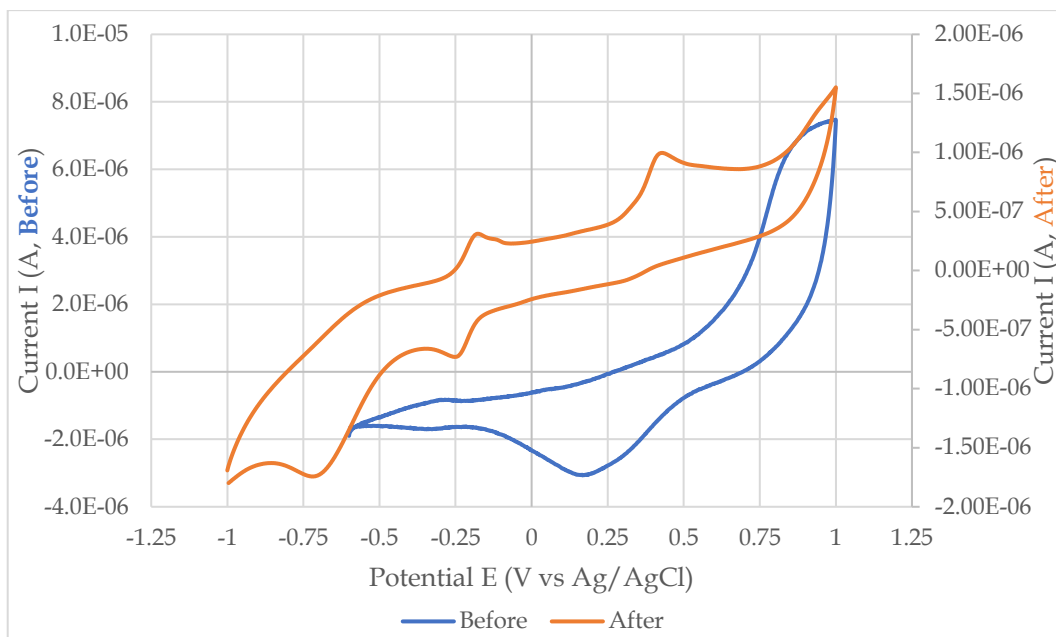


Figure 14: Cyclic voltammograms of 0.1 mM BQ(OH)₂ before and after irradiation on diode-array spectrophotometer. Scan is ramped from -1 to +1 V vs RE in positive direction with 100 mV/s scan rates and 10 μA current sensitivity range at 25 °C.

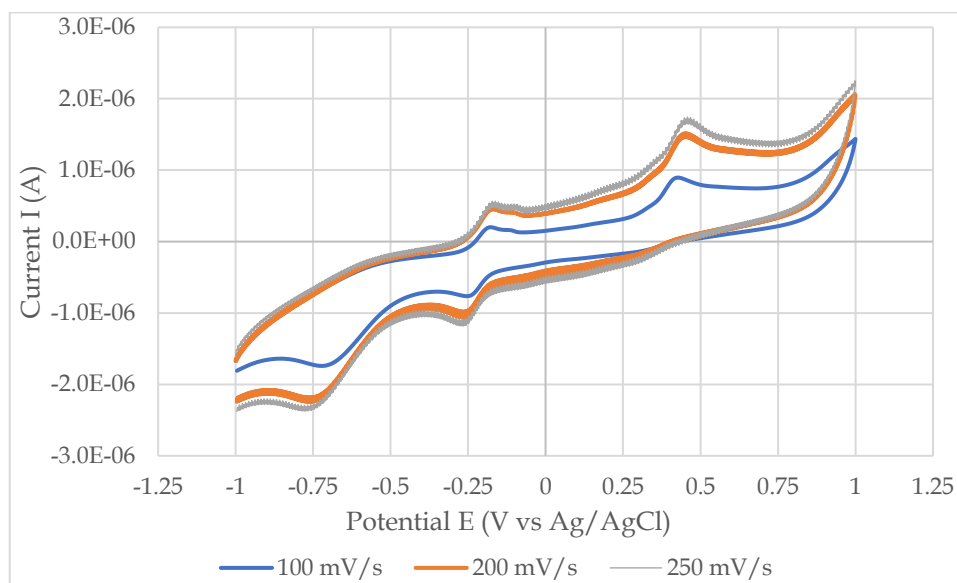


Figure 15: Effect of change in scan rate on CV of 0.1 mM BQ(OH)₂. Scan is ramped from -1 to +1 V vs RE in positive direction with 5 μA current sensitivity range at 25 °C.

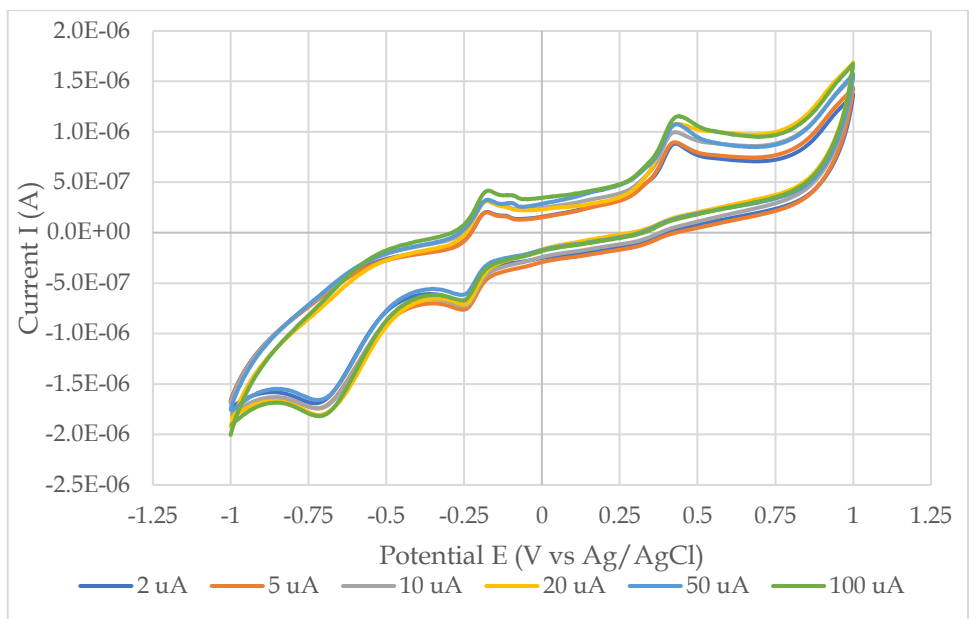


Figure 16: Effect of change in current sensitivity range on CV of 0.1 mM BQ(OH)₂. Scan is ramped from -1 to +1 V vs RE in positive direction with 100 mV/s scan rates at 25 °C.

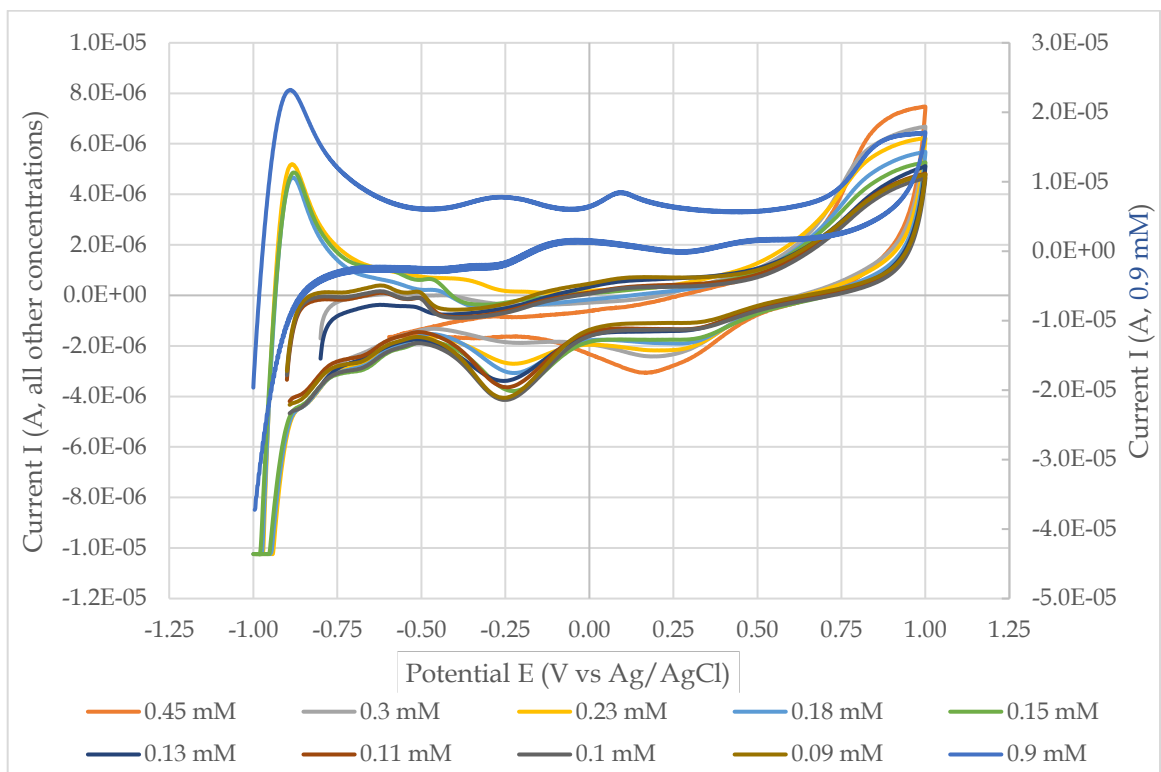


Figure 17: Effect of change in concentration on CV of 1.0 mM BQ(OH)₂ stock solution diluted and measured for CV until signal disappeared. Scan is ramped from -1 to +1 V vs RE in positive direction with 100 mV/s scan rates and 10 μ A current sensitivity range at 25 °C.

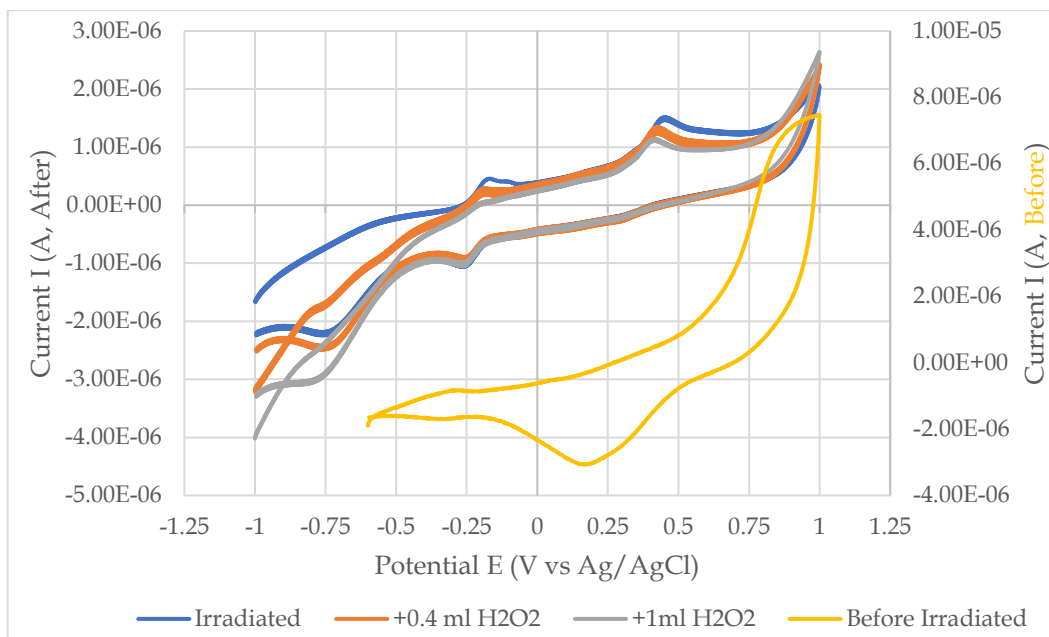


Figure 18: Effect of 3% H₂O₂ on irradiated BQ(OH)₂ in comparison to before irradiation. Scan is ramped from -1 to +1 V vs RE in positive direction with 200 mV/s scan rates and 5μA current sensitivity range at 25 °C.

Figure 18 is quite interesting: it depicts the effect of H₂O₂ on CV of irradiated BQ(OH)₂. We can infer that the window we are using is still not quite wide enough to see the redox reactions happening here. We cannot see a new peak after the addition of H₂O₂. However, CV in comparison to the one before irradiation shows that after addition of H₂O₂ to the irradiated BQ(OH)₂ solution, the reactant peak started to disappear at -0.75 V. At the same time, the products at peak currents at +0.40 V (hydroxyquinone) and -0.30 were not changed substantially. Only a very small amount of product is formed after such a short reaction time. Reaction is still quite slow here. As it is known from earlier literature data, increasing the pH and/or the BQ(OH)₂ and H₂O₂ concentrations would be a good strategy to accelerate the oxidation reaction.

Chapter 4. Summary

It is now very important for us to preserve the environment and secure energy from renewable energy sources (wind, hydropower, solar, geothermal, and biomass) for growing populations. Solar energy offers a great alternative to fossil fuels. My thesis is aimed at possible utilization of solar energy by benzoquinone derivatives that also have their great importance in biological systems.

We have known photodiodes to redox flow batteries throughout the development of devices for capturing solar energy. Benzoquinones already have their special application in photo-chemical reactions and flow batteries. The aim of my research is to find the right substituent among benzoquinones and derive its redox and photochemical properties by which we can increase the efficiency of flow batteries by combining their redox properties and photo-sensitivity.

In my experiments, I investigated the redox and photochemical properties of hydroxy derivative of benzoquinone (2,5-dihydroxy-1,4-benzoquinone) using two analytical methods: spectrophotometry and cyclic voltammetry. This derivative of benzoquinones was chosen because it was not examined earlier in depth for its photochemical properties especially for its application to redox flow battery. Benzoquinone solution was photo-decomposed on a diode-array spectrophotometer and analysed with spectrophotometry as well as with cyclic voltammetry to see the photo-decomposed products.

Iron-copper redox couple was studied electro-analytically as a comparison redox model for photo-decomposed benzoquinone redox system. The change of CN⁻ ion complexation situation was derived theoretically for the iron-copper redox system.

We concluded that iron and copper have readily measurable voltammograms. Their standard redox potentials are +0.609 and +0.302 (for iron and copper respectively) which were calculated from peak potentials. It was found that increasing scan rate just increase intensity of anodic and cathodic peak without any change in half-potential values. The same was true for the benzoquinone derivative. In the case of iron-copper redox couple, under the given conditions, copper dominated in voltammogram and masked the iron peaks. But in the case of

FeCl₃ and CuSO₄, we got a double peak in between positive peak of Cu²⁺ and negative peak of Fe³⁺. We found that redox potentials will be affected substantially by the ligands in the solution even if we keep the metal ions same or metal ion pair (two different oxidation states).

The photo-decomposition of 2,5-dihydroxy-1,4-benzoquinone was quite slow, and we got only 3.8% conversion after one hour of illumination on diode-array spectrophotometer. Even with this small amount of photo-decomposition, we were able to see formation of hydroxyquinone and quinone/hydroquinone products in voltammogram of irradiated 2,5-dihydroxy-1,4-benzoquinone.

From the previously published research, it has been known that some quinone derivatives are not well soluble in aqueous solution. We must study many quinone derivative from solubility, spectroscopic properties, redox and kinetically for developing a right choice for quinone derivative for flow batteries chargeable by solar energy. All these properties should be studied comparatively which is a way forward.

Acknowledgement

First and foremost, I would like to praise Allah the Almighty, the Most Gracious, and the Most Merciful for His countless blessings over me throughout my life and especially in completing this piece of work.

I would like to express my sincere gratitude to my supervisor Dr. Katalin Ósz for inspiring my interest to the fascinating field of Photochemistry. I acknowledge her continuous mentoring, guidance, and support throughout the work.

I am truly thankful to Dr. András Kiss for his help in learning the electrochemistry lab instruments. I am also thankful to Dr. Gábor Lente for letting me learn multi-component equilibriums through MEDUSA software theoretically. In addition, my greatest gratitude and appreciation are addressed to Dr. Gábor Lente, Dr. László Kollár, Dr. Ferenc Kilar, Dr. Attila Felinger and all other faculty teachers whose combined devotion and sincerity in teaching allowed me to comprehend and write this small piece of work. Amongst a multitude of other things, you have provided me with a wealth of knowledge that I will value for the rest of my life.

I am very thankful to “Stipendium Hungaricum” program for giving me full grant to study B.Sc. Chemistry at this university. Many thanks to all my colleagues and friends with whom I have worked during my years as an undergraduate student.

Most importantly, I would like to thank my wonderful family for believing in me and supporting me throughout my life and education. Thank you to my mother, for all that I cannot put into words!

Pécs, May 2022.

Muhammad Zahid Nazir

Reference list

- (1) Lau, D.; Song, N.; Hall, C.; Jiang, Y.; Lim, S.; Perez-Wurfl, I.; Ouyang, Z.; Lennon, A. Hybrid Solar Energy Harvesting and Storage Devices: The Promises and Challenges. *Mater. Today Energy* **2019**, *13*, 22–44. <https://doi.org/10.1016/j.mtener.2019.04.003>.
- (2) Wang, Y.; Zhong, W. H. Development of Electrolytes towards Achieving Safe and High-Performance Energy-Storage Devices: A Review. *ChemElectroChem* **2015**, *2* (1), 22–36. <https://doi.org/10.1002/celec.201402277>.
- (3) Lenaz, G.; Fato, R.; Formiggini, G.; Genova, M. L. The Role of Coenzyme Q in Mitochondrial Electron Transport. *Mitochondrion* **2007**, *7* (SUPPL.), 8–33. <https://doi.org/10.1016/j.mito.2007.03.009>.
- (4) Müh, F.; Glöckner, C.; Hellmich, J.; Zouni, A. Light-Induced Quinone Reduction in Photosystem II. *Biochim. Biophys. Acta - Bioenerg.* **2012**, *1817* (1), 44–65. <https://doi.org/10.1016/j.bbabi.2011.05.021>.
- (5) Berger, S.; Hertl, P.; Rieker, A. Physical and Chemical Analysis of Quinones. *The Quinonoid Compounds (1988)*. April 27, 1988, pp 29–78. <https://doi.org/https://doi.org/10.1002/9780470772119.ch2>.
- (6) Horiuchi, S.; Kumai, R.; Tokura, Y. Hydrogen-Bonded Donor-Acceptor Compounds for Organic Ferroelectric Materials. *Chem. Commun.* **2007**, No. 23, 2321–2329. <https://doi.org/10.1039/b617881b>.
- (7) Kitagawa, S.; Kawata, S. Coordination Compounds of 1,4-Dihydroxybenzoquinone and Its Homologues. Structures and Properties. *Coord. Chem. Rev.* **2002**, *224* (1–2), 11–34. [https://doi.org/10.1016/S0010-8545\(01\)00369-1](https://doi.org/10.1016/S0010-8545(01)00369-1).
- (8) Huskinson, B.; Marshak, M. P.; Suh, C.; Er, S.; Gerhardt, M. R.; Galvin, C. J.; Chen, X.; Aspuru-Guzik, A.; Gordon, R. G.; Aziz, M. J. A Metal-Free Organic-Inorganic Aqueous Flow Battery. *Nature* **2014**, *505* (7482), 195–198. <https://doi.org/10.1038/nature12909>.
- (9) Gan, D. Aqueous Photochemistry of 1,4-Benzoquinones and Their Possible Role in the Photochemistry of Natural Organic Matter, Doctoral Dissertation, University of Maryland, 2005.

- (10) Chambers, J. Q. Electrochemistry of Quinones. *The Quinonoid Compounds* (1988). April 27, 1988, pp 719–757.
<https://doi.org/https://doi.org/10.1002/9780470772119.ch12>.
- (11) Józsa, É.; Kiss, V.; Ósz, K. Photochemical Processes of 1,4-Benzoquinones in Aqueous Medium. *J. Photochem. Photobiol. A Chem.* **2018**, *360* (December 2017), 166–173. <https://doi.org/10.1016/j.jphotochem.2018.04.024>.
- (12) Pochon, A.; Vaughan, P. P.; Gan, D.; Vath, P.; Blough, N. V.; Falvey, D. E. Photochemical Oxidation of Water by 2-Methyl-1,4-Benzoquinone: Evidence against the Formation of Free Hydroxyl Radical. *J. Phys. Chem. A* **2002**, *106* (12), 2889–2894. <https://doi.org/10.1021/jp012856b>.
- (13) Paulsen, H. Cyclic Voltammetry - "Electrochemical Spectroscopy." *Angew. Chemie Int. Ed. English* **1982**, *21* (3), 155–173.
- (14) Nicholson, R. S. Theory and Application of Cyclic Voltammetry for Measurement of Electrode Reaction Kinetics. *Anal. Chem.* **1965**, *37* (11), 1351–1355. <https://doi.org/10.1021/ac60230a016>.
- (15) DuVall, S. H.; McCreery, R. L. Control of Catechol and Hydroquinone Electron-Transfer Kinetics on Native and Modified Glassy Carbon Electrodes. *Anal. Chem.* **1999**, *71* (20), 4594–4602.
<https://doi.org/10.1021/ac990399d>.
- (16) Bond, A. M.; Feldberg, S. W. Analysis of Simulated Reversible Cyclic Voltammetric Responses for a Charged Redox Species in the Absence of Added Electrolyte. *J. Phys. Chem. B* **1998**, *102* (49), 9966–9974.
<https://doi.org/10.1021/jp9828437>.
- (17) Dev, K.; Kaur, R.; Vashisht, G.; Sulania, I.; Annapoorni, S. Magnetization Reversal Behavior in Electrodeposited Fe-Co-Ni Thin Films. *IEEE Trans. Magn.* **2022**, *1*. <https://doi.org/10.1109/TMAG.2022.3159562>.
- (18) Heffner, J. E.; Wigal, C. T.; Moe, O. A. Solvent Dependence of the One-Electron Reduction of Substituted Benzo- And Naphthoquinones. *Electroanalysis* **1997**, *9* (8), 629–632.
<https://doi.org/10.1002/elan.1140090810>.
- (19) Skyllas-Kazacos, M.; Chakrabarti, M. H.; Hajimolana, S. A.; Mjalli, F. S.;

- Saleem, M. Progress in Flow Battery Research and Development. *J. Electrochem. Soc.* **2011**, *158* (8), R55. <https://doi.org/10.1149/1.3599565>.
- (20) Hruska, L. W.; Savinell, R. F. Investigation of Factors Affecting Performance of the Iron-redox Battery. *J. Electrochem. Soc.* **1981**, *128* (1), 18.
- (21) Kabtamu, D. M.; Lin, G. Y.; Chang, Y. C.; Chen, H. Y.; Huang, H. C.; Hsu, N. Y.; Chou, Y. S.; Wei, H. J.; Wang, C. H. The Effect of Adding Bi³⁺ on the Performance of a Newly Developed Iron-Copper Redox Flow Battery. *RSC Adv.* **2018**, *8* (16), 8537–8543. <https://doi.org/10.1039/c7ra12926b>.
- (22) Kwabi, D. G.; Lin, K.; Ji, Y.; Kerr, E. F.; Goulet, M. A.; De Porcellinis, D.; Tabor, D. P.; Pollack, D. A.; Aspuru-Guzik, A.; Gordon, R. G.; Aziz, M. J. Alkaline Quinone Flow Battery with Long Lifetime at PH 12. *Joule* **2018**, *2* (9), 1894–1906. <https://doi.org/10.1016/j.joule.2018.07.005>.
- (23) Yang, B.; Hooper-Burkhardt, L.; Krishnamoorthy, S.; Murali, A.; Prakash, G. K. S.; Narayanan, S. R. High-Performance Aqueous Organic Flow Battery with Quinone-Based Redox Couples at Both Electrodes. *J. Electrochem. Soc.* **2016**, *163* (7), A1442–A1449. <https://doi.org/10.1149/2.1371607jes>.
- (24) Oliveira, P.; Faria, R. B. The Chlorate - Iodine Clock Reaction. **2005**, 18022–18023.
- (25) Fábíán, I.; Lente, G. Light-Induced Multistep Redox Reactions: The Diode-Array Spectrophotometer as a Photoreactor. *Pure Appl. Chem.* **2010**, *82* (10), 1957–1973. <https://doi.org/10.1351/PAC-CON-09-11-16>.
- (26) BURGESS, C. The Role of Photodiode Array Spectrometry in Analytical Chemistry. In *Advances in Standards and Methodology in Spectrophotometry*; Burgess, C., Mielenz, K. D. B. T.-A. S. L., Eds.; Elsevier, 1987; Vol. 2, pp 303–324. <https://doi.org/https://doi.org/10.1016/B978-0-444-42880-6.50020-9>.
- (27) Lente, G.; Espenson, J. H. Photoreduction of 2,6-Dichloroquinone in Aqueous Solution: Use of a Diode Array Spectrophotometer Concurrently to Drive and Detect a Photochemical Reaction. *J. Photochem. Photobiol. A Chem.* **2004**, *163* (1–2), 249–258. <https://doi.org/10.1016/j.jphotochem.2003.12.005>.
- (28) Józsa, É.; Jenei, L. B.; Kégl, T.; Ósz, K. Substituent Effects on the Activation Parameters of the Reaction between 1,4-Benzoquinones and Hydrogen

- Peroxide: A Combined Experimental and Theoretical Study. *J. Mol. Struct.* **2022**, *1261*, 132916. <https://doi.org/10.1016/j.molstruc.2022.132916>.
- (29) Lukács, P. A Nátrium-Antrakinon-2-Szulfonát Fotokémiai Vizsgálata (Photochemical Study of Sodium Anthraquinone-2-Sulfonate), BSc Thesis, University of Pécs, 2022.
- (30) Ignasi Puigdomenech. MEDUSA, KTH Royal Institute of Technology, Stockholm, Sweden <https://www.kth.se/che/medusa/>.

List of abbreviations

AQDS	9,10-Anthraquinone-2,7-disulfonic acid
BQ	1,4-Benzoquinone
BQ(OH)	Hydroxyquinone (Hydroxybenzoquinone)
BQ(OH)₂	2,5-Dihydroxy-1,4-benzoquinone
CE	Counter electrode
CV	Cyclic Voltammetry
DCQ	2,6-Dichloro-1,4-benzoquinone
H₂Q	Hydroquinone (Benzene-1,4-diol or Quinol)
<i>i</i>_{pa}	Anodic current
<i>i</i>_{pc}	Cathodic current
MEDUSA	Making equilibrium diagrams using sophisticated algorithms
OD	Outer diameter
RE	Reference electrode
RFB	Redox flow battery
SHE	Standard hydrogen electrode
UV	Ultraviolet
Vis	Visible
WE	Working electrode

Appendixes

Appendix A (Voltammograms)

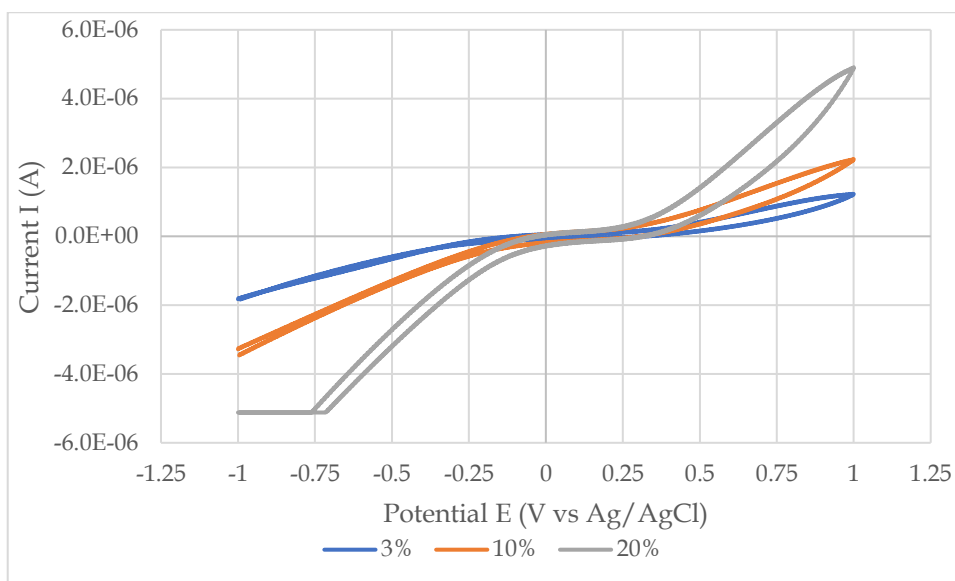


Figure 19: Voltammograms of different concentrations of H₂O₂. Scan is ramped from -1 to +1 V vs RE in positive direction with 250 mV/s scan rates and 5 μ A current sensitivity range at 25 °C.

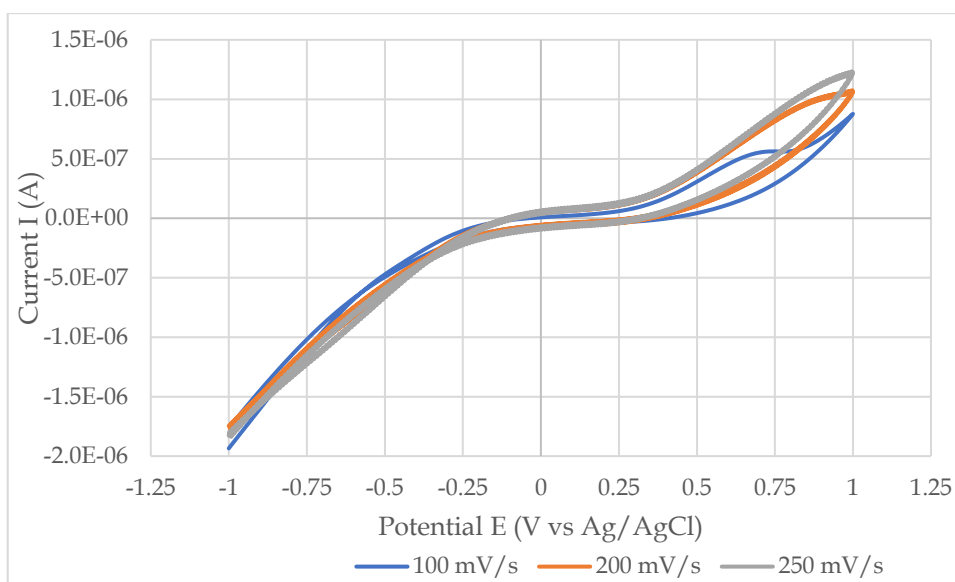


Figure 20: Effect of change in scan rate on CV of 3% H₂O₂. Scan is ramped from -1 to +1 V vs RE in positive direction with 5 μ A current sensitivity range at 25 °C.

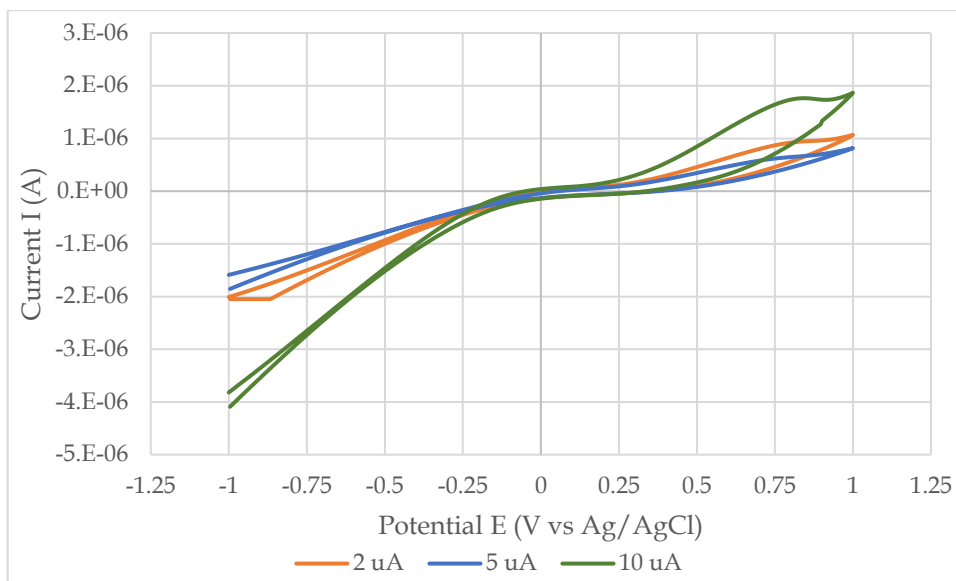


Figure 21: The Effect of change in current sensitivity range on CV of 10% H₂O₂. Scan is ramped from -1 to +1 V vs RE in positive direction with 100 mV/s scan rates at 25 °C

**Declaration
of the originality of the writing**

(According to Code of Studies and Examinations of the University of Pécs, Annex nr. 14/1.)

I, the undersigned, **Nazir, Muhammad Zahid**, NEPTUN system identifier: **VOBJDP**, declare under penalty of perjury

that every part of my writing,

Redox, kinetic, and photochemical properties of 2,5-dihydroxy-1,4-benzoquinone and other model systems

is the result of my own, autonomous work, I only used referred sources (special literature, tools, etc.) and I observed the pertaining rules of the University of Pécs while preparing my writing.

I am aware that the University of Pécs has the right to check the observation of copyright rules through a plagiarism tracing system.

Pécs, May 9, 2022



.....
signature of the student